

American Journal of Ophthalmology
Peripheral Macular Endothelial Dystrophy: Clinical, Histopathologic, Genetic and Functional Characterization
--Manuscript Draft--

Manuscript Number:	AJO-25-222R3
Article Type:	Original Article
Keywords:	Corneal endothelial dystrophy, CHST6, keratan sulfate
Corresponding Author:	Anthony Aldave, MD UCLA Jules Stein Eye Institute Los Angeles, CA United States
First Author:	Wenlin Zhang
Order of Authors:	Wenlin Zhang Huong Duong, MD Passara Jongkhajornpong, MD Do Thi Thuy Hang, MD Huan Pham, MD Mai Nguyen, MD Charlene Choo, MD Dominic Williams, MD Xuan Nguyen, MD Tien Dat Nguyen, MD Brian Aguirre Shaukat Khan, PhD Madhuri Wadehra, PhD Shunji Tomatsu, MD, PhD Anthony Aldave, MD
Abstract:	<p>Objective To report a CHST6-associated corneal endothelial dystrophy.</p> <p>Design Prospective observational case series.</p> <p>Participants Thirty-five individuals from seven families, including 13 affected individuals exhibiting corneal epithelial and stromal edema, peripheral posterior corneal macular opacities, and endothelial guttae, as well as 22 unaffected family members.</p> <p>Methods Whole-exome sequencing was performed in three families and Sanger sequencing of CHST6 was performed in all individuals. Histological examination of Descemet membrane (DM) excised at the time of endothelial keratoplasty was performed for three probands. Serum keratan sulfate (KS) levels were measured in members of six families. Functional analysis of identified mutations was performed using CHST6 promoter containing CHST6 expression vector in human keratocytes (HK) and corneal endothelial cells (HCEnC).</p>

	<p>Main Outcome Measures</p> <p>Clinical phenotype; genetic analysis; functional analysis of identified CHST6 mutations; serum KS levels; histologic examinations of DM.</p>
	<p>Results</p> <p>All affected individuals demonstrated peripheral macular opacities at the level of DM. Visually significant corneal edema in affected individuals was successfully managed by endothelial keratoplasty. Genetic analysis demonstrated a rare CHST6 promoter mutation (c.-690G>C) in the homozygous state in affected individuals from three families and in the compound heterozygous state with a CHST6 coding mutation (p.R211Q, p.Y268C or p.P280L) in affected individuals from the other four families. In silico analysis predicted c.-690G>C to be a regulatory variant, located at the RNA polymerase II binding site. Functional analysis in vitro demonstrated that c.-690G>C leads to increased KS sulfation the corneal endothelium and DM, with no change of KS sulfation in keratocytes. Histologic examination of DM from affected individuals revealed elevated levels of sulfated and non-sulfated KS in DM and endothelium, consistent with the functional analysis. Minimum changes in serum sulfated KS levels were observed in affected individuals.</p>
	<p>Conclusions</p> <p>We suggest the name Peripheral macular endothelial dystrophy (PMED) to describe this dystrophy that is characterized by peripheral posterior corneal macular opacities and endothelial dysfunction without stromal haze or opacities. Given that both PMED and macular corneal dystrophy are associated with promoter and coding region mutations in CHST6, we propose that they be categorized as CHST6-associated corneal dystrophies.</p>
Suggested Reviewers:	<p>Andrew J.W. Huang Washington University in St Louis huangandrew@nospam.wustl.edu</p> <p>Walter Lisch Johannes Gutenberg Universitat Mainz prof.dr.lisch@augenklinik-hanau.de</p>
Opposed Reviewers:	
Response to Reviewers:	<p>July 16, 2025</p> <p>Richard K. Parrish, II, MD Editor in Chief, American Journal of Ophthalmology</p> <p>RE: AJO-25-222, "Peripheral Macular Endothelial Dystrophy: Clinical, Histopathologic, Genetic and Functional Characterization"</p> <p>Dear Dr. Parrish:</p> <p>Thank you for considering our manuscript for publication and giving us the opportunity to respond to the reviewers' comments.</p> <p>Submitted Design section in the Abstract: Design: Observational case series.</p> <p>Suggested Design section for the Abstract: Design: Prospective observational case series.</p> <p>ABSTRACT. The Design has been modified to include the word "Prospective".</p> <p>The Methods section of the paper should also be updated with this description of the design. For example, "Approval for this prospective observational case series" rather than "Approval for this study".</p>

MATERIALS AND METHODS. Page 5. Line 56. The text has been revised to include the suggested, more accurate, description of the study design.

Other comments from the reviewers:

Reviewer #2: It is a interesting manuscript. It was for me a very interesting discussion with the senior author of the manuscript.

During this discussion I remembered Goethe's Faust: "Man errs as long he strives."

The third version of IC3D was published in CORNEA in 2024. We have further a lot of open questions. The fourth version of IC3D will probably appear in about 8 -10 years.

We can hope that we can than subdivide the MCD into "CHST6 epithelial, stromal and endothelial corneal dystrophies." This will then include "CHST6 associated corneal dystrophy."

I propose for the future to get a concordance between the different spots (maculae) and the genetical evaluation.

Once again, we need the support of the molecular pathophysiologists and geneticists to better understand the diagnostic complexity of the different forms of corneal dystrophy.

However, "Genotypes need Phenotypes." We will never get the full answer !

It is very interesting and that is why I agree with the proposal "CHST6 associated corneal dystrophy" for the publication in The American Journal of Ophthalmology.

The authors greatly appreciate Reviewer 2's insightful comments.

Reviewer #3: The authors have thoroughly and precisely addressed all requested changes and comments.

Referring to the condition as a CHST6-associated corneal dystrophy represents, in my view, a well-balanced and appropriate compromise.

I have no further remarks and recommend the article for publication.

The authors are very pleased that we and the reviewers agree on the suggested classification of the condition that we describe as a CHST6-associated corneal dystrophy.

Sincerely,

Anthony J. Aldave, M.D.
Professor of Ophthalmology
Bartly J. Mondino, M.D., Endowed Chair in Ophthalmology
Vice Chair for Academics
Co-Chief, Cornea and Uveitis Division
Director, Cornea and Refractive Surgery Fellowship
The Stein Eye Institute

ABSTRACT

Objective: To report a *CHST6*-associated corneal endothelial dystrophy.

Design: Prospective observational case series.

Participants: Thirty-five individuals from seven families, including 13 affected individuals exhibiting corneal epithelial and stromal edema, peripheral posterior corneal macular opacities, and endothelial guttae, as well as 22 unaffected family members.

Methods: Whole-exome sequencing was performed in three families and Sanger sequencing of *CHST6* was performed in all individuals. Histological examination of Descemet membrane (DM) excised at the time of endothelial keratoplasty was performed for three probands. Serum keratan sulfate (KS) levels were measured in members of six families. Functional analysis of identified mutations was performed using *CHST6* promoter containing *CHST6* expression vector in human keratocytes (HK) and corneal endothelial cells (HCEnC).

Main Outcome Measures: Clinical phenotype; genetic analysis; functional analysis of identified *CHST6* mutations; serum KS levels; histologic examinations of DM.

Results: All affected individuals demonstrated peripheral macular opacities at the level of DM. Visually significant corneal edema in affected individuals was successfully managed by endothelial keratoplasty. Genetic analysis demonstrated a rare *CHST6* promoter mutation (c.-690G>C) in the homozygous state in affected individuals from three families and in the compound heterozygous state with a *CHST6* coding mutation (p.R211Q, p.Y268C or p.P280L) in affected individuals from the other four families. *In silico* analysis predicted c.-690G>C to be a regulatory variant, located at the RNA polymerase II binding site. Functional analysis *in vitro* demonstrated that c.-690G>C

leads to increased KS sulfation the corneal endothelium and DM, with no change of KS sulfation in keratocytes. Histologic examination of DM from affected individuals revealed elevated levels of sulfated and non-sulfated KS in DM and endothelium, consistent with the functional analysis. Minimum changes in serum sulfated KS levels were observed in affected individuals.

Conclusions: We suggest the name Peripheral macular endothelial dystrophy (PMED) to describe this dystrophy that is characterized by peripheral posterior corneal macular opacities and endothelial dysfunction without stromal haze or opacities. Given that both PMED and macular corneal dystrophy are associated with promoter and coding region mutations in *CHST6*, we propose that they be categorized as *CHST6*-associated corneal dystrophies.

UNIVERSITY OF CALIFORNIA, LOS ANGELES

UCLA

BERKELEY • DAVIS • IRVINE • LOS ANGELES • RIVERSIDE • SAN DIEGO • SAN FRANCISCO



SANTA BARBARA • SANTA CRUZ

JULES STEIN EYE INSTITUTE
DAVID GEFFEN SCHOOL OF MEDICINE AT UCLA
100 STEIN PLAZA
LOS ANGELES, CA 90095

July 16, 2025

Richard K. Parrish, II, MD
Editor in Chief, *American Journal of Ophthalmology*

RE: AJO-25-222, "Peripheral Macular Endothelial Dystrophy: Clinical, Histopathologic, Genetic and Functional Characterization"

Dear Dr. Parrish:

Thank you for considering our manuscript for publication and giving us the opportunity to respond to the reviewers' comments.

Submitted Design section in the Abstract:
Design: Observational case series.

Suggested Design section for the Abstract:
Design: Prospective observational case series.

ABSTRACT. The Design has been modified to include the word "Prospective".

The Methods section of the paper should also be updated with this description of the design. For example, "Approval for this prospective observational case series" rather than "Approval for this study".

MATERIALS AND METHODS. Page 5. Line 56. The text has been revised to include the suggested, more accurate, description of the study design.

Other comments from the reviewers:

Reviewer #2: It is a interesting manuscript. It was for me a very interesting discussion with the senior author of the manuscript.

During this discussion I remembered Goethe's Faust: "Man errs as long he strives."

The third version of IC3D was published in CORNEA in 2024. We have further a lot of open questions. The fourth version of IC3D will probably appear in about 8 -10 years.

We can hope that we can than subdivide the MCD into "CHST6 epithelial, stromal and endothelial corneal dystrophies." This will then include "CHST6 associated corneal dystrophy."

I propose for the future to get a concordance between the different spots (maculae) and the genetical evaluation.

Once again, we need the support of the molecular pathophysiologists and geneticists to better understand the diagnostic complexity of the different forms of corneal dystrophy.

However, "Genotypes need Phenotypes." We will never get the full answer !

It is very interesting and that is why I agree with the proposal "CHST6 associated corneal dystrophy" for the publication in The American Journal of Ophthalmology.

The authors greatly appreciate Reviewer 2's insightful comments.

Reviewer #3: The authors have thoroughly and precisely addressed all requested changes and comments.

Referring to the condition as a CHST6-associated corneal dystrophy represents, in my view, a well-balanced and appropriate compromise.

I have no further remarks and recommend the article for publication.

The authors are very pleased that we and the reviewers agree on the suggested classification of the condition that we describe as a CHST6-associated corneal dystrophy.

Sincerely,

Anthony J. Aldave, M.D.

Professor of Ophthalmology

Bartly J. Mondino, M.D., Endowed Chair in Ophthalmology

Vice Chair for Academics

Co-Chief, Cornea and Uveitis Division

Director, Cornea and Refractive Surgery Fellowship

The Stein Eye Institute

[Click here to view linked References](#)1 Zhang et al. Peripheral macular endothelial dystrophy 1
2
34 **Peripheral Macular Endothelial Dystrophy: Clinical, Histopathologic, Genetic and**
5
6 **Functional Characterization**
7
8 3 Short title: Peripheral Macular Endothelial Dystrophy
9
10
11
12 4 Wenlin Zhang, M.D., Ph.D.,^a Huong Duong, M.D.,^b Passara Jongkajornpong, M.D., Ph.D.,^c
13
14 5 Do Thi Thuy Hang, M.D.,^d Huan Pham, M.D.,^b Mai Nguyen, M.D.,^b Charlene Choo, M.D.,^a
15
16 6 Dominic Williams, M.D.,^a Xuan Nguyen, M.D.,^e Tien Dat Nguyen, M.D.,^e Brian Aguirre,^f
17
18
19 7 Shaukat Khan, Ph.D.,^g Madhuri Wadehra, Ph.D.,^f Shunji Tomatsu, M.D., Ph.D.,^g and Anthony
20
21 8 J. Aldave, M.D.^{a#}
22
23
24 9 ^a Stein Eye Institute, UCLA, Los Angeles CA.
25
26 10 ^b Ho Chi Minh City Eye Hospital, Ho Chi Minh City, Vietnam.
27
28
29 11 ^c Department of Ophthalmology, Faculty of Medicine Ramathibodi Hospital, Mahidol
30
31 12 University, Bangkok, Thailand
32
33
34 13 ^d Vietnam National Eye Hospital, Hanoi, Vietnam.
35
36 14 ^e University of Medicine and Pharmacy at Ho Chi Minh City, Ho Chi Minh City, Vietnam.
37
38
39 15 ^f Department of Pathology and Laboratory Medicine, UCLA, Los Angeles, CA.
40
41 16 ^g Nemours Children's Health, Wilmington, DE.
42
43
44
45 17 Supplemental Material available at AJO.com
46
47
48 18 **#Correspondence**
49
50
51 19 Anthony J. Aldave, M.D.
52
53
54 20 Stein Eye Institute, David Geffen School of Medicine at UCLA, 200 Stein Plaza, UCLA, Los
55
56 21 Angeles, CA 90095-7003
57
58 22 Tel: 310-206-7202
59
60 23 aldave@jsei.ucla.edu
61
62
63
64
65

KEYWORDSCorneal endothelial dystrophy, *CHST6*, keratan sulfate

26 INTRODUCTION

27 The corneal dystrophies are a group of inherited disorders that are typically bilateral,
28 symmetric, slowly progressive and are not influenced by environmental or systemic factors¹.
29 Traditionally, corneal dystrophies have been anatomically classified, based on the layer of the
30 cornea that is primarily affected: epithelium, Bowman layer, stroma and endothelium.
31 However, the International Committee for the Classification of the Corneal Dystrophies has
32 reclassified the dystrophies according to the cellular origin of the dystrophic deposits, and
33 thus the *TGFB1* dystrophies are now classified as epithelial-stromal dystrophies.² In the case
34 of macular corneal dystrophy (MCD), although histopathologic examination demonstrates
35 non-sulfated/low-sulfated glycosaminoglycans (GAG) in both the stroma and the
36 endothelium, it remains classified as a stromal dystrophy due to the presence of macular
37 stromal deposits and diffuse stromal haze that characterize MCD and the absence of
38 evidence of endothelial dysfunction in affected individuals.

39 MCD is associated with mutations in the *CHST6* gene, encoding corneal N-
40 acetylglucosamine-6-O-sulfotransferase (CGn6ST or GlcNAc6ST), which plays an essential
41 role in the sulfation of GAG in the cornea by catalyzing the transfer of sulfate from 3'-
42 phosphoadenosine 5'-phosphosulfate to position 6 of a non-reducing N-acetylglucosamine
43 (GlcNAc) residue in keratan sulfate (KS). Decreased CGn6ST/GlcNAc6ST activity in the
44 corneal keratocytes in individuals with MCD leads to the accumulation of Alcian blue-positive
45 non-sulfated/low-sulfated GAG deposits (decreased sulfation of KS) within keratocytes and in
46 the extracellular corneal stroma, resulting in loss of corneal clarity.

47 In the current study, we describe a corneal endothelial dystrophy that is characterized by
48 peripheral posterior corneal macular opacities reminiscent of those associated with MCD, but
49 without the macular stromal deposits and diffuse stromal haze that are essential phenotypic

2 features of MCD. Given this, the development of corneal edema in symptomatic individuals
3 and the successful restoration of vision with endothelial keratoplasty as well as the functional
4 impact of the associated *CHST6* promoter mutation, we propose the classification of this
5 dystrophy, which we have named Peripheral macular endothelial dystrophy (PMED), and
6 MCD as *CHST6*-associated corneal dystrophies.

7
8
9
10
11
12
13
14

15
16
17
18
19
20
21
22
23
24

25
26
27
28
29
30
31
32
33
34

35
36
37
38
39

40
41
42
43
44

45
46
47
48
49

50
51
52
53
54

55
56
57
58
59

60
61
62
63
64
65

2
3
4
5
MATERIALS AND METHODS6
7
8 Approval for this observational case series was obtained from the Institutional Review Board
9 at the University of California at Los Angeles (UCLA IRB#11–000020). Written informed
10 consent was obtained from all subjects in this study according to the tenets of the Declaration
11 of Helsinki.
12
13
1415
16
17 *Clinical Evaluation*18
19
20 All affected and unaffected individuals from seven families who agreed to participate in the
21 study underwent a comprehensive ophthalmic examination (Fig. 1), including slit lamp
22 biomicroscopy and photography, ultrasound biomicroscopy (UBM), Scheimpflug imaging
23 (Oculus Pentacam), and anterior segment optical coherence tomography (AS-OCT). The
24 diagnosis of PMED was established based on the presence of round, gray-white, discrete
25 deposits confined to the peripheral Descemet membrane (DM) or posterior surface of the
26 cornea, without stromal opacities or haze and with or without corneal epithelial and/or stromal
27 edema.
28
29
30
31
32
33
34
35
36
37
3839
40
41 *Sanger Sequencing of CHST6*42
43
44 After obtaining informed consent, saliva and/or blood samples were collected from members
45 of each of the seven families using a saliva collection kit (Oragene, DNA Genotek, Inc.) or a
46 standard phlebotomy procedure. Genomic DNA was isolated from saliva samples using the
47 Oragene Purifier (OG-L2P, DNA Genotek, Inc.) and from blood samples using the FlexiGene
48 DNA Kit (QIAGEN), according to the manufacturer's instructions. Each of the three exons of
49 *CHST6* and the 2.5 kb region upstream of exon 1 were amplified by PCR and sequenced
50 using Sanger sequencing (Supplemental Materials, Primers and PCR conditions used for
51 *CHST6* screening) (Supplemental Table 1). Sequences were compared to the wild-type
52
53
54
55
56
57
58
59
60
61
62
63
64
65

2
3
4 CHST6 gene transcript (NM_021615), and the minor allele frequencies (MAF) of identified
5 variants were obtained from public databases including Exome Aggregation Consortium
6 (ExAC), 1000 Genomes Project (1000Genome), Trans-Omics for Precision Medicine
7 (TOPMED) and Genome Aggregation Database (gnomAD). A rare variant was defined as a
8 variant with MAF < 0.01 in all databases.
9
10
11
12
13
14
15
16
17
18

19 *Whole Exome Sequencing (WES) and Data Analysis*

20 WES was performed on the genomic DNA of all enrolled members from PMED families A, B,
21 and C (Fig. 1). DNA libraries were prepared using the TruSeq DNA Sample Preparation Kit
22 v2 (Illumina Inc.), and exome capture was performed with the SeqCap EZ Exome Library
23 v2 (Roche NimbleGen, Inc.). Paired-end sequencing (2×150 bp) was carried out on
24 Illumina's HiSeq 3000 platform. The generated raw sequence reads were aligned to Genome
25 Research Consortium human build 38 (GRCh38) using Burrows-Wheeler Aligner (BWA) in
26 maximal exact match (MEM) mode and subsequently processed following the Genome
27 Analysis Toolkit (GATK) best practice guidelines for variant calling (Supplemental Materials,
28 GATK variant calling). After variant calling, common variants (MAF > 0.01) were filtered out,
29 and rare variants were annotated using the Ensembl Variant Effect Predictor (VEP) online
30 tool. Coding non-synonymous variants and splice site variants were retained and analyzed
31 for segregation with the affected status in Family C using both autosomal recessive and
32 autosomal dominant models, and genes containing potentially pathogenic variants were
33 subsequently screened in members of Families B and C (Supplemental Materials, WES
34 variant filtration).

35 *In silico variant prediction and scoring*

36 The identified CHST6 coding variants were analyzed using the online tools PredictSNP2 and

2
3 PolyPhen-2 to assess their potential impact on protein function.^{3,4} PredictSNP2 is a
4 consensus classifier that combines five prediction methods, including Combined Annotation
5
6 Dependent Depletion (CADD), Deleterious Annotation of Genetic Variants using Neural
7 Networks (DANN), Functional Analysis through Hidden Markov Models (FATHMM), FunSeq2
8 and Genome Wide Annotation of Variants (GWAVA).³ The identified *CHST6* promoter
9 variants were analyzed using the online tool RegulomeDB to determine the likelihood of each
10 variant being in a regulatory region bound by subunits of transcriptional machinery and/or
11 transcriptional factors.⁵ The RegulomeDB score represents a model that integrates functional
12 genomics features, including continuous values from multiple databases such as chromatin
13 immunoprecipitation sequencing (ChIP-seq) signal and DNase-seq signal from The
14 Encyclopedia of DNA Elements (ENCODE), information content change, and predicted
15 scores from the deep learning sequence-based algorithmic program DeepSEA.^{6,7}

16 *In vitro CHST6 functional assay*

17 For the functional assay, we generated a *CHST6* expression vector containing the native
18 promoter of *CHST6*. Briefly, a 1439 bp fragment encompassing exon 1 of the *CHST6* gene,
19 the predicted *CHST6* promoter and two adjacent enhancers (identified based on ENCODE
20 registry of candidate cis-regulatory elements (cCREs)), was cloned into the previously
21 described *CHST6* expression vector pcDNA3-CGn6ST.^{8,9} The cloning replaced the
22 sequences of CMV enhancer-containing promoter and T7 promoter. The pcDNA3-CGn6ST
23 vector contains the nucleotide sequences of exons 2 and 3 of the *CHST6* gene. The newly
24 cloned *CHST6* native promoter-containing *CHST6* expression vector was named pcDNA3-
25 CGn6STwPro and contained the wild-type sequences of the non-coding 5' region, the non-
26 coding exons 1 and 2, and the entire coding sequence of exon 3 of the *CHST6* gene. Site-
27 directed mutagenesis was then performed on pcDNA3-CGn6STwPro, also denoted as
28
29
30
31
32
33
34
35
36
37
38
39
40
41
42
43
44
45
46
47
48
49
50
51
52
53
54
55
56
57
58
59
60
61
62
63
64
65

2 CGn6STwPro_WT, to generate nucleotide changes consistent with the mutations found in
3 PMED pedigrees (QuikChange Lightning Site-Directed Mutagenesis Kit, Agilent
4 Technologies). The following three single mutant constructs were created: CGn6STwPro_c.-
5 690G>C, CGn6STwPro_Y268C (nucleotide change c.803A>G), and CGn6STwPro_P280L
6 (nucleotide change c.839C>T). Additionally, exon 1 of the *CHST6* gene along with
7 surrounding sequences (1439 bp) from the proband of family B was cloned into pcDNA3-
8 CGn6ST using the same method as described above. This generated pcDNA3-
9 CGn6STwPro_PT, which contained three adjacent variants (c.[-668C>T; -690G>C; -
10 792C>T]). All mutations were confirmed by Sanger sequencing (Laragen, Inc., Culver City,
11 CA).

12 To investigate the functional impact of the identified *CHST6* mutations in human

13 corneal endothelial cells and keratocytes, telomerase immortalized human corneal
14 endothelial cells (HCEnC) and keratocytes (HK) were transfected with wild-type and/or
15 mutant CHST6 promoter-containing expressing vectors (CGn6STwPro) using
16 Lipofectamine® LTX with PLUS reagent (A12621, Life Technologies) according to the
17 manufacturer's recommendations (Supplemental Materials, Human corneal endothelial cell
18 line cell culture, Human corneal keratocyte cell culture).^{10,11} To enhance the detection of
19 sulfated KS, HCEnC or HK (seeded in 24-well plates at 50% confluence 24 hours prior) were
20 co-transfected with expression vectors b3GnT7 (250 ng/well) and HKSG6ST (250 ng/well),
21 two enzymes involved in the extension of KS and C-6 sulfation of Gal residue in KS, along
22 with CGn6STwPro wild-type and/or mutant (250 ng/well). To simulate compound
23 heterozygous *CHST6* mutations identified in some affected individuals, an equal amount of
24 two CGn6STwPro mutant constructs (125 ng/well) were used. A total of 750 ng of plasmid
25 DNA was used per well.

149 The following combination of CGn6STwPro constructs were used to mimic the *CHST6*
150 mutation status observed in individuals reported here: 1) WT/WT, representing the healthy
151 control without *CHST6* mutations; 2) PT/PT, representing affected individuals with
152 homozygous variant c.[-668C>T; -690G>C; -792C>T] in Families B, E, and G; 3) PT/P280L,
153 mimicking the proband of Family A with compound heterozygous variants c.[-668C>T; -
154 690G>C; -792C>T] and the previously unreported P280L; 4) PT/Y268C, mimicking the
155 affected individuals in Family C with compound heterozygous variants c.[-668C>T; -690G>C;
156 -792C>T] and Y268C; 5) WT/PT, mimicking the affected mother of the proband (I-2) in Family
157 A with heterozygous variant c.[-668C>T; -690G>C; -792C>T]; 6) c.-690G>C/c.-690G>C
158 (CGn6STwPro_c.-690G>C), assessing the impact of isolated homozygous variant c.-690G>C
159 without two adjacent variants c.-668C>T and c.-792C>T; 7) c.-690G>C/P280L, assessing the
160 impact of compound heterozygous variants c.-690G>C and P280L; 8) c.-690G>C/Y268C,
161 assessing the impact of compound heterozygous variants c.-690G>C and Y268C; 9)
162 P280L/P280L (CGn6STwPro_P280L), assessing the impact of homozygous variant P280L;
163 and 10) Y268C/Y268C (CGn6STwPro_Y268C), assessing the impact of homozygous variant
164 Y268C on CGn6ST/CHST6 enzymatic function.

165 The enzymatic activities of CGn6ST, together with b3GnT7 and HKSG6ST, result in
166 highly sulfated KS, which can be detected by the 5D4 antibody (MABN2483, Millipore
167 Sigma). Forty-eight hours post-transfection, cells were lysed with radioimmunoprecipitation
168 assay (RIPA) buffer containing proteinase and phosphatase inhibitors. Total protein was
169 quantified using the bicinchoninic acid (BCA) assay, separated and detected using a
170 capillary-based Western Blot system (Simple Western assay Wes, ProteinSimple). Highly
171 sulfated KS, b3GnT7 protein and GAPDH were detected using 5D4, anti-B3GNT7 (NBP1-
172 69637, Novus Biological) and anti-GAPDH (MAB374, Millipore Sigma) antibodies,

2
3 respectively. Quantification and data analysis were performed using the Compass for Simple
4 Western software (ProteinSimple). The level of 5D4-positive sulfated KS was normalized to
5 GAPDH as the loading control and then to B3GNT7 as an internal control for transfection
6 efficiency in each sample. Four biological replicates of transfection and Western Blot were
7 performed, and the average 5D4+ KS level was calculated for each CHST6 mutant or
8 combination of mutants.

9 *Histology and Immunofluorescence Staining*

10 Five-micrometer sections of paraffin-embedded corneas from seven healthy donors, surgical
11 DM specimens from three probands from families A, C, and F, and a surgical DM specimen
12 from an individual with pseudophakic corneal edema (PCE) were deparaffinized and
13 rehydrated in a graded ethanol series (100%, 95%, 70% and 50%).

14 H&E staining of specimens was performed following a standardized protocol
15 (Translational Pathology Core Laboratory, Department of Pathology, UCLA). For Alcian blue
16 staining, the rehydrated sections were stained with an Alcian blue solution (1% Alcian blue in
17 3% acetic acid in deionized water; pH = 2.5) for 30 minutes, followed by staining with a 0.5%
18 aqueous neutral red solution for 2 minutes. For high iron diamine staining, the rehydrated
19 sections were stained with a high iron diamine solution (0.24% N, N-dimethyl-meta-
20 phenylenediamine dihydrochloride, 0.04% N, N-dimethyl-para-phenylenediamine
21 dihydrochloride, 2.8% Ferric Chloride in deionized water) for 18 hours, followed by staining
22 with a 0.5% aqueous neutral red solution for 2 minutes. H&E, Alcian Blue or high iron diamine
23 stained sections were imaged with a KEYENCE BZ-X700 all-in-one fluorescence microscope.

24 For 5D4 staining, the rehydrated sections underwent antigen retrieval in 10 mM sodium
25 citrate, followed by a standard immunofluorescence staining protocol with the 5D4 antibody

2 overnight at 4°C and Alexa 568 anti-mouse secondary antibody with DAPI. For Lectin-FITC
3 staining, the rehydrated sections underwent antigen retrieval in a citrate-based antigen
4 unmasking solution (Vector Labs, #H-3300) for 25 minutes, followed by a standard
5 immunofluorescence staining protocol with Lectin-FITC conjugated antibody (Vector
6 Laboratories, #FL-1171). 5D4 and Lectin-FITC stained sections were imaged with an inverted
7 confocal fluorescence microscope (Olympus FV-1000, Olympus Corporation).

8 *Sulfated Glycosaminoglycan Measurement in Serum and/or Dried Blood Spots*

9 The sulfation levels of serum GAG, including dermatan sulfate (DS), heparan sulfate (HS),
10 and KS, were measured by liquid chromatography with tandem mass spectrometry (LC-
11 MS/MS) as previously described and the results were compared with age-matched
12 controls.^{12,13} Serum samples were collected from 17 individuals and dried blot spots (DBS)
13 were collected from 10 individuals from the seven families (Fig. 1).

14 *Calculation of Odds of Pathogenicity (Odds Path) for Identified Variants*

15 The number of criteria met for each identified *CHST6* variant was counted as N for each
16 criterion subtype, including benign supporting (BP1–6), benign strong (BS1–4), benign stand-
17 alone (BA1), pathogenic supporting (PP1–5), pathogenic moderate (PM1–6), pathogenic
18 strong (PS1–4), or very strong (PVS1). The odds of pathogenicity (*OddsPath*) of each variant
19 was calculated using the following published formula *OddsPath* =

$$20 \quad 350 \left(\frac{N_{PP}}{8} + \frac{N_{PM}}{4} + \frac{N_{PS}}{2} + \frac{N_{PVS}}{1} - \frac{N_{BP}}{8} - \frac{N_{BS}}{2} \right)^{14}$$

21 The Bayesian posterior probability was calculated by the
22 equation $Post_P = \frac{OddsPath * Prior_P}{(OddsPath - 1) * Prior_P + 1}$, in which prior probability (*Prior_P*) by default is 0.1.

23 *Post_P* was then assigned a variant classification as follows: benign < 0.001; 0.001 ≤ likely
24 benign < 0.1; 0.1 ≤ Variant of Uncertain Significance (VUS) < 0.90; 0.90 ≤ likely pathogenic <

3 18 0.99; 0.99 ≤ pathogenic.¹⁵ OddsPath cut-off scores for Supporting, Moderate, Strong, and
45 19 Very Strong pathogenic evidence were obtained from published guidelines.¹⁶
6

7

8

9

10

11

12

13

14

15

16

17

18

19

20

21

22

23

24

25

26

27

28

29

30

31

32

33

34

35

36

37

38

39

40

41

42

43

44

45

46

47

48

49

50

51

52

53

54

55

56

57

58

59

60

61

62

63

64

65

4 **RESULTS**5 **Clinical Features**6 *7 Family A*

8
9 A 47-year-old Thai woman (Fig. 1. A. II-2) with an unremarkable past medical history
10 presented with progressive decrease in vision in both eyes. Corrected visual acuities (CVA)
11 measured 20/40 OD and 20/50 OS. Slit lamp biomicroscopy and AS-OCT revealed inferior
12 paracentral corneal subepithelial fibrosis, underlying stromal edema and multiple discrete
13 gray peripheral opacities at the level of DM, predominantly located in the superior and inferior
14 peripheral cornea (Fig. 2A, Supplemental Fig. 1A). Central corneal pachymetry measured
15 626 µm OD and 604 µm OS. A combined Descemet membrane endothelial keratoplasty
16 (DMEK), cataract extraction was performed in each eye with restoration of stromal clarity
17 other than for residual inferior paracentral subepithelial scarring (Fig. 2B). Slit lamp
18 examination of other family members revealed similar appearing discrete gray opacities only
19 in the proband's 73-year-old mother, whose CVA measured 20/70 OU (Fig. 1. A. I-2). As the
20 opacities in proband's mother were confined to the inferior peripheral cornea in each eye,
21 were significantly fewer in number, and were not associated with corneal edema (Fig. 2C),
22 her decreased corrected visual acuity was attributed to bilateral severe nuclear sclerosis. The
23 other examined family members, including the proband's father (Fig. 1. A. I-1), older sister
24 (Fig. 1. A. II-1), and daughter (Fig. 1. A. III-1), demonstrated clear corneas.
25
26

27 *Family B*

28 A 49-year-old Vietnamese woman (Fig. 1. B. II-1) with an unremarkable past medical history
29 presented with glare, halo, and foreign body sensation in both eyes (OD > OS) that was
30 worse in the morning. Slit lamp biomicroscopy revealed mild diffuse corneal stromal edema
31
32

2
3
4 OD and trace stromal edema OS with multiple discrete grayish peripheral opacities at the
5 level of DM in both eyes (Fig. 2D). The patient complained of progressive loss of vision
6 thereafter for 6 months as CVA declined from 20/100 to counting finger (CF) at 2 meters OD
7 and from 20/20 to 20/25 OS. Slit lamp biomicroscopy revealed temporal microcystic epithelial
8 and stromal edema extending to the central cornea in both eyes (Fig. 2E). Central corneal
9 pachymetry measured by UBM was 620 μm OU. A combined Descemet stripping automated
10 endothelial keratoplasty (DSAEK), cataract extraction was performed in the right eye, and the
11 central cornea remained clear 2 years (Fig. 2F) and 4 years later with CVA of 20/25 and
12 20/30, respectively. The unoperated left eye developed progressive subepithelial scarring
13 and stromal edema with CVA decreasing to CF at 3 meters.

13
14 The parents of the proband (Fig. 1. B. I-1 and B. I-2), who are first cousins, were not
15 available for examination. The proband's younger brother (Fig. 1. B. II-2), who was diagnosed
16 with Fuchs endothelial corneal dystrophy and progressive moderate glaucoma, underwent
17 two DSAEK procedures and tube shunt placement twice in the left eye. Postoperative CVA in
18 the left eye was limited to hand motion due to glaucomatous optic neuropathy. In the
19 unoperated right eye, CVA measured 20/30. Trace peripheral corneal stromal edema and a
20 few peripheral grey macular deposits at the level of DM were observed (Fig. 2G), with central
21 and peripheral corneal pachymetry measuring 570 μm and 830-970 μm , respectively.
22
23 Examination of the proband's son (Fig. 1. B. III-1) revealed a clear cornea in each eye.

24
25
26 *Family C*

27
28
29 A 60-year-old Vietnamese man (Fig. 1. C. II-5) presented with decreased vision in the left
30 eye. Slit lamp examination revealed fine peripheral gray-white opacities at the level of the DM
31 and central guttae in the right eye, and fine central epithelial edema, moderate stromal
32

2 edema and DM folds in the left eye (Fig. 2H). CVA measured 20/70 OD and CF at 1 meter
3 OS, while central pachymetry measured 457 µm OD and 602 µm OS. A combined DMEK,
4 cataract extraction was performed in the left eye, with the restoration of a clear cornea (Fig.
5 2I). Examination of the proband's 72-year-old sister (Fig. 1. C. II-1) revealed similar
6 appearing white macular deposits, more profound in size and number, primarily located in the
7 superior and inferior posterior peripheral cornea in both eyes (Fig. 2J). Trace corneal stromal
8 edema was present in both eyes with central corneal pachymetry measuring 551 µm OD and
9 532 µm OS. Eight other family members who were examined demonstrated clear corneas
10 (Fig. 1. C). The parents of the proband, who were third cousins, were deceased and their
11 medical records were not available.

12
13
14
15
16
17
18
19
20
21
22
23
24
25
26
27
28
29
30
31
32
33
34
35
36
37
38
39
40
41
42
43
44
45
46
47
48
49
50
51
52
53
54
55
56
57
58
59
60
61
62
63
64
65

Family D

32 A 41-year-old Vietnamese man (Fig. 1. D. II-1) presented with blurred vision and foreign body
33 sensation, worse in the morning, in both eyes (OS > OD) for two years. Corrected visual
34 acuity measured 20/25 OD and 20/50 OS. Slit lamp biomicroscopy revealed moderate diffuse
35 stromal edema, 3+ endothelial guttae and peripheral grey-white discrete opacities at the level
36 of the DM in both eyes (Fig. 3A). Central corneal pachymetry measured by Pentacam for the
37 central 0-2 mm zone was 505 – 522 µm OD and 545 - 742 µm OS and AS-OCT revealed
38 stromal edema and DM folds in the left eye (Fig. 3B). Examination of the proband's 36-year-
39 old brother (Fig. 1. D. II-3) revealed no stromal edema, central 2 mm guttae, and a few fine
40 opacities in the peripheral superior posterior cornea of the right eye. His left eye
41 demonstrated focal inferior paracentral corneal epithelial and stromal edema, and a few
42 discrete grey macular opacites at the level of DM in the superior and nasal periphery (Fig.
43 3C). Examination of the proband's 31-year-old brother (Fig. 1. D. II-5) revealed a few discrete
44

4 gray posterior stromal opacities bilaterally, located only in superior peripheral cornea, without
5 corneal edema (Fig. 3D). Eight other family members who were examined demonstrated
6 clear corneas (Fig. 1. D).

7

8 *Family E*

9

10 A 54-year-old Vietnamese woman (Fig. 1. E. II-1) presented with a progressive decrease in
11 vision and foreign body sensation in both eyes for four years. CVA measured CF at 0.2 meter
12 OD and at 0.5 meter OS. Slit lamp examination revealed central corneal epithelial bullae,
13 diffuse moderate stromal edema, and fine peripheral grey macular deposits at the level of
14 DM, primarily in the superior and inferior peripheral cornea, in both eyes (Fig. 3E). AS-OCT
15 imaging revealed corneal epithelial and stromal edema in both eyes, and central corneal
16 thickness measured 685 – 696 µm OD and 715 µm OS using AS-OCT (Supplemental Fig.
17 31)

18 1B). The proband's 42-year-old younger sister (Fig. 1. E. II-2) had CVA of CF at 0.2 meters
19 OD and CF at 0.6 meters OS secondary to epithelial bullae, subepithelial fibrosis and stromal
20 edema in both eyes (Fig. 3F). Central corneal pachymetry measured 851 µm OD and 836 µm
21 OS using AS-OCT (Supplemental Fig. 1C).

22

23 *Family F*

24

25 A 64-year-old Vietnamese man (Fig. 1. F. I-1) presented with a two-year history of declining
26 vision in both eyes, with CVA decreasing from 20/40 to 20/100 in the right eye and from
27 20/100 to hand motion in the left eye. Slit lamp biomicroscopy revealed fine grey-white
28 peripheral opacities at the level of the DM in both eyes (Fig. 3G). Focal inferior epithelial and
29 diffuse mild stromal edema were present in the right cornea, while diffuse epithelial edema,
30 subepithelial fibrosis and severe stromal edema were present in the left eye. Central corneal
31 pachymetry measured 700 µm OD and 1100 µm OS using UBM. DSEK was performed in the
32

2
3 left eye, after which the corneal edema improved to trace stromal edema and CVA improved
4
5 to counting finger at 1 meter (Fig. 3H).
6
7

8
9 **314 Family G**
10
11

12
13 A 58-year-old Vietnamese man (Fig. 1. G. I-1) presented for evaluation of white deposits in
14 both corneas diagnosed 7 years prior. CVA measured 20/20 OD and 20/25 OS. Slit lamp
15 examination revealed grey-white macular deposits at the level of the DM in both eyes. While
16 the deposits in the paracentral cornea were discrete, they coalesced into confluent opacities
17 on the peripheral posterior cornea of each eye (Fig. 3I).
18
19

20 **320 Genetic Analysis**
21
22

23
24 Identified CHST6 promoter mutation c.-690G>C, in homozygous state or in compound
25 heterozygous state with a coding region mutation, segregated with affected status in seven
26 families
27
28

29
30 The macular appearance of the peripheral opacities in affected individuals prompted
31 screening of the coding and putative promoter regions of the CHST6 gene. A rare promoter
32 mutation n.-97G>C, c.-690G>C (GRCh38.p14 chr16: g.75495538C>G, rs1009794816,
33 GnomAD MAF 0.000064), was identified in all affected individuals in either a homozygous
34 state or in a compound heterozygous state with a CHST6 coding mutation, with the exception
35 of the affected mother of the proband in Family A (Fig. 1. A. I-2) (Table 1). This individual,
36 who displayed a milder corneal phenotype with few deposits and no corneal edema, was
37 heterozygous for the c.-690G>C mutation without a coding region mutation. The affected
38 proband in Family A was compound heterozygous for c.-690G>C and a novel coding region
39 mutation c.839C>T, p.(Pro280Leu) (GRCh38.p14 chr16: g.75478990G>A, rs201767298, no
40
41
42
43
44
45
46
47
48
49
50
51
52
53
54
55
56
57
58
59
60
61
62
63
64
65

2
3 MAF) while unaffected individuals were heterozygous for either mutation. In Family B, E, and
4 G, affected individuals were homozygous and unaffected individuals were heterozygous for
5
6 the c.-690G>C mutation. In Family C, affected individuals were compound heterozygous for
7
8 c.-690G>C with a rare coding mutation c.803A>G, p.(Tyr268Cys) (GRCh38.p14 chr16:
9 g.75479026T>C, rs72547539, GnomAD MAF 0.000064), whereas unaffected individuals
10
11 were heterozygous for one of the two mutations. In Families D and F, affected individuals
12
13 were compound heterozygous for c.-690G>C with a rare coding mutation c.632G>A,
14
15 p.(Arg211Gln) (GRCh38.p14 chr16: g.75479197C>T, rs771397083, GnomAD MAF
16
17 0.000004), while unaffected individuals were heterozygous for one of the two mutations.
18
19

20 Two common promoter variants adjacent to c.-690G>C mutation, c.-792C>T
21
22 (GRCh38.p14 chr16: g.75495640G>A, rs2550322, TOPMED MAF 0.034) and c.-668C>T
23
24 (GRCh38.p14 chr16: g.75495516G>A, rs2550323, TOPMED MAF 0.114) were identified in
25
26 all individuals with the c.-690G>C mutation and were confirmed to be on the same allele (*in*
27
28 *cis*) as c.-690G>C. The three adjacent variants *in cis* are denoted as c.[-668C>T; -690G>C; -
29
30 792C>T]. In regards to the large deletion and rearrangement of *CHST6* upstream region
31
32 previously associated with MCD type II¹⁷, a heterozygous deletion was identified in only one
33
34 of the probands, in family A (Fig. 1. A. II-2).
35
36

37
38 **451 Whole Exome Sequencing fails to identify other candidate genes associated with PMED**
39
40

41 All enrolled individuals from Families A, B, and C underwent WES. Assuming an
42
43 autosomal recessive inheritance in Family C, homozygous or compound heterozygous
44
45 candidate variants that segregated with affected status in Family C were identified in *SND1*,
46
47 *ANKRD36* and *TAS2R43*. However, no candidate variant within these genes segregated with
48
49 the affected status in Families A and B (Supplemental Table 2). Assuming an autosomal
50
51

2
3 dominant inheritance in Family C, heterozygous candidate variants that segregated with
4 affected status in Family C were identified in *CFAP74*, *FAAP20*, *PRDM16*, *CHD5*, *GRB14*,
5
6
7
8 *NUP210*, *ZNF860*, *FAM160A1*, *FAM186A*, *PDIA3* and *NCOA6*. However, no candidate
9 variant within these genes segregated with the affected status in Families A and B, excluding
10 mutations in these genes as the genetic basis of PMED in each of these families
11
12
13 (Supplemental Table 3).
14
15
16

17
18
19 *CHST6 promoter variant c.-690G>C is predicted to be a regulatory variant bound by RNA*
20
21 *polymerase II*
22
23
24

25 *In silico* analysis using RegulomeDB predicted that c.-690G>C is a regulatory variant with a
26 score of 1 on a scale of 0 to 1 (Table 2). This prediction is based on experimental data
27 deposited in the ENCODE database, which includes information on transcriptional factor (TF)
28 binding peaks, DNase footprint, DNase peaks, and the presence of TF binding motif
29 (consensus genomic sequences that specifically bind TF). Among the available ChIP-seq
30 data, the most frequently bound TF or subunit of transcriptional machinery at the genome
31 coordinate of c.-690G>C was RNA polymerase II subunit A (POL2A), observed in 10 out of
32 36 data sets. POL2A is the largest subunit of RNA polymerase II, responsible for synthesizing
33 messenger RNA in eukaryotes. The identified common variants c.-792C>T and c.-668C>T
34 were predicted to be moderately likely regulatory variants with scores of 0.61 and 0.56,
35 respectively (Table 2). *In silico* analysis of the three identified coding variants, p.Arg211Gln,
36 p.Tyr268Cys and p.Pro280Leu, predicted all to be “Deleterious” in PredictSNP2 and
37 “Probably Damaging” in PolyPhen-2 (Table 2).
38
39
40
41
42
43
44
45
46
47
48
49
50
51
52
53
54
55
56
57
58
59
60
61
62
63
64
65

60 *CHST6 c.-690G>C leads to increased sulfated KS in human corneal endothelial cells but not*
61 *in human keratocytes*

2
3 To assess the functional effects of the identified *CHST6* variants, wild-type and/or mutant
4
5 *CHST6* promoter-containing expressing vectors (CGn6STwPro) were transfected into
6
7 immortalized HCEnC and HK (Fig. 4A). In HCEnC, Western Blot results showed low levels of
8
9 5D4+ KS in cells transfected with wild-type *CHST6* expression construct (WT/WT). However,
10
11 increased levels of 5D4+ KS were observed following transfection with either c.-690G>C
12
13 promoter variant-containing construct (PT/PT or c.-690G>C/c.-690G>C), regardless of dose.
14
15 The increase in 5D4+ KS was evident in HCEnC transfected under all conditions with c.-
16
17 690G>C promoter variant, including PT/PT, c.-690G>C/c.-690G>C, PT/P280L, PT/Y268C,
18
19 WT/PT, c.-690G>C/P280L, or c.-690G>C/Y268C conditions. However, the levels of 5D4+ KS
20
21 remained unchanged in HCEnC following transfection of only coding variant-containing
22
23 constructs P280L/P280L and Y268C/Y268C (Fig. 4B, C).

24
25 In HK, on the contrary, there was significantly higher 5D4+ KS in cells transfected with
26
27 wild-type *CHST6* expression construct (WT/WT) compared to HCEnC WT/WT transfection.
28
29 There was no change in 5D4+ KS level following transfection with c.-690G>C promoter
30
31 variant-containing constructs under PT/PT, c.-690G>C/c.-690G>C, PT/P280L, PT/Y268C,
32
33 and WT/PT conditions, compared to HK transfected with WT/WT. Transfection in HK with
34
35 coding variant-containing constructs, including c.-690G>C/P280L, c.-690G>C/Y268C,
36
37 P280L/P280L, and Y268C/Y268C conditions, led to decreased 5D4+ KS levels compared to
38
39 HK transfected with WT/WT. The above data suggested an aberrant 5D4+ KS
40
41 overexpression in HCEnC is induced by the presence of *CHST6* c.-690G>C promoter variant,
42
43 and the previously unreported *CHST6* P280L mutation leads to decreased CGn6ST/*CHST6*
44
45 enzymatic activity in HK, similar to the previously reported Y268C mutation (Fig. 4B, C).

46
47
48
49
50
51
52
53
54
55
56
57
58
59
60
61 *CHST6* c.-690G>C induced increase of sulfated and unsulfated KS is restricted to Descemet
62
63 membrane and corneal endothelium

2 To investigate whether the aberrant overexpression of 5D4+ KS was the cause of corneal
3 endothelial changes observed in affected individuals in our case series, we performed
4 immunohistochemical staining of three DM samples collected during DMEK surgery of
5 probands of Families A, C and F. A full thickness donor cornea and a DM sample from an
6 individual with pseudophakic corneal edema (PCE) were included as controls. Staining
7 performed included H&E staining, immunofluorescence staining with 5D4 antibody for highly
8 sulfated KS, FITC conjugated Lectin (Lectin-FITC) for non-sulfated KS, Alcian Blue staining
9 for non-sulfated KS and High Iron Diamine (HID) staining for low sulfated KS (Fig. 5). On
10 H&E staining, the DM samples from the three probands showed various degrees of DM
11 thickening and dystrophic appearing cornea endothelial cells, with areas devoid of cells.
12

13 Immunofluorescence staining with the 5D4 antibody revealed increased staining of 5D4+ KS
14 throughout the full thickness of DM in the three probands, displaying a lamellated appearance
15 compared to controls. This lamellated appearance suggested that 5D4+ KS was continuously
16 deposited by the corneal endothelial cells over time. Lectin-FITC staining was also increased
17 in the DM samples from the three probands compared to the controls, with a laminated
18 appearance throughout the thickness of DM, particularly in the posterior zone/layers closer to
19 the corneal endothelium. A tumor tissue sample with neovascularization included as a
20 positive control for Lectin-FITC demonstrated staining of blood vessel basement membranes.
21 Alcian Blue staining demonstrated positive staining primarily in the posterior zone/layers of
22 the DM and in the cytoplasm of the remaining corneal endothelial cells in the three DM
23 samples. In contrast, control samples showed no Alcian Blue staining of the DM or corneal
24 endothelium. A sample of human colon adenocarcinoma included as a positive control
25 showed Alcian blue positive mucus droplets within colon epithelial cells. HID staining was
26 observed in corneal endothelial cells and/or in protruding nodules on the posterior surface of
27

2
3 DM in the three DM samples, whereas no HID staining was observed in controls, suggesting
4
5 that the gray deposits on the posterior aspect of the peripheral cornea observed clinically
6
7 may consist of low sulfated KS. A sample of healthy murine colon epithelium included as
8
9 positive control for HID staining demonstrated dark brown HID-stained mucus droplets within
10
11 the colon epithelial cells.
12
13

14 To evaluate the impact of the *CHST6* c.-690G>C mutation on systemic KS sulfation and
15 metabolism, serum and/or DBS were collected from affected and unaffected members of 6 of
16
17 7 families (Fig. 1). Control samples included serum samples from four healthy individuals, the
18
19 unrelated spouse of the proband in Family E, and two individuals with fleck corneal
20
21 dystrophy. The levels of di-sulfated KS, mono-sulfated KS, total sulfated KS (di-sulfated KS +
22
23 mono-sulfated KS), dermatan sulfate (DS), and heparan sulfate (HS) from serum samples
24
25 and DBS samples for each individual are presented in Tables 3 and 4, respectively. Adjusted
26
27 DBS measurements were provided for ease of comparison with serum sample
28
29 measurements, based on a previously published method.¹³ The blood sulfated KS levels in
30
31 most of the individuals examined, affected or unaffected, were within the range of sulfated KS
32
33 levels found in health controls.
34
35

36 The above data suggested that the aberrant overexpression of 5D4+ high sulfated KS
37 induced by the *CHST6* c.-690G>C mutation was restricted to the corneal endothelium and
38 DM in the corneas of affected individuals. Additionally, low-sulfated KS and non-sulfated KS
39
40 were overexpressed in corneal endothelium and DM as well.
41
42

43 *CHST6* c.-690G>C is a pathogenic variant

44
45 To determine the pathogenicity of the identified variants, we followed established guidelines
46
47 published by American College of Medical Genetics and Genomics (ACMG), Association for
48
49

2
3 Molecular Pathology (AMP) and UK Association for Clinical Genomic Science (ACGS). These
4 guidelines include the 2015 ACMG-AMP variant interpretation guidelines for Mendelian
5 disorders¹⁸, the 2018 ACMG/AMP guideline update for PP5 and BP6 variants¹⁹, the Bayesian
6 adaptation of the ACMG/AMP variant interpretation framework¹⁴, the 2020 ACMG/AMP
7 guideline update for PS3/BS3 criterion²⁰, and the 2022 ACGS variant interpretation guidelines
8 for non-coding variants.²¹ Four of the six identified variants, c.-690G>C, p.Arg211Gln,
9 p.Tyr268Cys, and p.Pro280Leu, can be classified as “Pathogenic”, each with a posterior
10 probability of 0.999 and a calculated OddsPath value of 13617, indicating that the pathogenic
11 evidence is “Very Strong” for all of these four variants (Table 5).

12

13

14

15

16

17

18

19

20

21

22

23

24

25

26

27

28

29

30

31

32

33

34

35

36

37

38

39

40

41

42

43

44

45

46

47

48

49

50

51

52

53

54

55

56

57

58

59

60

61

62

63

64

65

3
4 461 **DISCUSSION**
5

6 462 This study details the clinical, histopathologic, immunohistochemical and genetic features of a
7
8 463 *CHST6*-associated corneal endothelial dystrophy affecting seven unrelated families from
9
10 464 Vietnam and Thailand. The clinical presentation of this corneal endothelial dystrophy is
11
12 465 distinct from previously described corneal endothelial dystrophies, namely Fuchs endothelial
13
14 466 corneal dystrophy, congenital hereditary endothelial dystrophy, posterior polymorphous
15
16 467 corneal dystrophy and x-linked endothelial corneal dystrophy. We suggest the name
17
18 468 Peripheral macular endothelial dystrophy (PMED) to describe this dystrophy, given the similar
19
20 469 appearance of the peripheral gray-white deposits observed in PMED to those observed in
21
22 470 MCD. However, this dystrophy is sufficiently distinct from MCD in terms of clinical features,
23
24 471 surgical management, genetic basis, and the functional impact of associated mutations to be
25
26 472 considered as unique corneal dystrophy.
27
28

29 473 In terms of the clinical features, individuals with PMED initially present with discrete gray-
30
31 474 white deposits on the posterior aspect of the peripheral cornea, without stromal haze, stromal
32
33 475 opacities or associated visual symptoms. The peripheral deposits slowly increase in size and
34
35 476 number, extending in some individuals into the mid-peripheral cornea. Subsequently,
36
37 477 epithelial and/or stromal corneal edema can develop, which can be successfully managed
38
39 478 with endothelial keratoplasty.
40
41

42 479 Similar to MCD, PMED is associated with promoter and coding region mutations in *CHST6*.
43
44 480 Identified coding region mutations, p.Tyr268Cys (Y268C) and p.Arg211Gln (R211Q), have
45
46 481 been previously reported to be associated with MCD, suggesting these two coding mutations
47
48 482 lead to decreased CGn6ST/*CHST6* enzymatic activity.^{22 23} However, p.Pro280Leu (P280L)
49
50 483 is novel and has not been associated with MCD. In each of the seven families that we
51
52 484 describe, the rare *CHST6* promoter mutation c.-690G>C, not previously associated with
53
54
55
56
57
58
59
60
61
62
63
64
65

485 MCD, was identified in either the homozygous or compound heterozygous state. *In silico*
486 analysis suggests that *CHST6* c.-690G>C is located at the binding site of RNA polymerase II
487 in the *CHST6* promoter. In vitro functional analysis, together with DM histological findings and
488 serum KS measurement, suggest that the c.-690G>C mutation, either in the homozygous
489 state or in the compound heterozygous state with another *CHST6* coding mutation, leads to
490 increased CGn6ST-mediated sulfation of KS only in the corneal endothelium and minimally
491 affects the CGn6ST enzyme activity in keratocytes and other somatic cell types. Additionally,
492 our data suggests that *CHST6* c.-690G>C in the heterozygous state may be sufficient to
493 cause disease, given the observation of a few peripheral deposits without corneal edema in a
494 heterozygous individual and the in vitro functional analysis of c.-690G>C in heterozygous
495 state demonstrating increased CGn6ST-mediated KS sulfation in corneal endothelial cells.
496 The distinct functional effects of *CHST6* c.-690G>C in corneal endothelial cells versus in
497 keratocytes and other somatic cell types may be related to the variability of enhancer and
498 promoter usage across tissues and the highly tissue-specific effects of non-coding variants.
499 Because of such tissue-specific effects, the 2022 ACGS variant interpretation guidelines for
500 non-coding variants²¹ specified that functional assay(s) of identified non-coding variant(s)
501 need to be performed in disease-relevant tissues or cell types. In our study, functional assays
502 of identified *CHST6* non-coding (c.-690G>C) and coding (P280L and Y268C) mutations were
503 performed in HCEnC and HK using the same outcome measurement – the level of 5D4
504 antibody labeled highly sulfated KS. While the functional assay showed decreased 5D4+ KS
505 with the two *CHST6* coding mutations in HK and no apparent change of already low 5D4+ KS
506 in HCEnC, the assay also showed *CHST6* c.-690G>C enhanced 5D4+ KS in HCEnC with no
507 apparent effect in HK. These results provided strong evidence of the differential functional
508 consequences of *CHST6* c.-690G>C in keratocytes compared to corneal endothelium.

2 To the best of our knowledge, there have been three publications describing two individual
3 cases and a family with peripheral gray-white macular deposits at the level of DM. Chaurasia
4 et al. described a 67-year-old Indian woman who presented with corneal edema, guttae and
5 bilateral deposits at DM, scattered circumferentially in the peripheral cornea.²⁴ After a clinical
6 diagnosis of macular corneal dystrophy was made, without genetic confirmation, Descemet
7 stripping endothelial keratoplasty (DSEK) was performed in the left eye, with improvement of
8 20/50 preoperative visual acuity to 20/30. Histological examination in the excised DM
9 demonstrated Alcian blue-positive endothelial cells, consistent with the findings in the DM
10 from the three probands that we report. We previously described a 68-year-old Chinese man
11 with bilateral clear corneas, except for peripheral round gray-white discrete deposits at the
12 level of DM. Both eyes exhibited decreased central corneal thickness and normal endothelial
13 cell densities. CHST6 screening in this individual demonstrated two compound heterozygous
14 mutations *in trans* configuration: c.-26C>A, a non-coding mutation in exon 2 that created a
15 new upstream open reading frame (uORF'), predicted to attenuate translation efficiency of
16 the downstream main ORF; and c.803A>G, p.(Tyr268Cys), which is the same mutation
17 identified in Family C that we report. Serum KS levels were reduced compared to age-
18 matched controls, leading us to conclude that the diagnosis in this case was macular corneal
19 dystrophy type II.²⁵ However, when we performed an in vitro cell-based assay of the
20 compound heterozygous mutations identified in this individual, we observed increased
21 sulfated KS compared to wild type in HCEnC but no effect in HK (Supplemental Fig. 2),
22 similar to that observed with CHST6 c.-690G>C. Given this, and the absence of macular
23 stromal deposits and diffuse stromal haze that are essential phenotypic features of MCD, we
24 now believe that this individual more likely has PMED. Ye et al. described a Chinese
25 pedigree consisting of 13 members across 3 generations, including 6 affected individuals,
26

2 showing an autosomal dominant inheritance pattern.²⁶ The average age of disease onset was
3 16.5 years of age, and affected members demonstrated progressive enlargement and
4 coalescence of white translucent spots initially confined to the peripheral DM with subsequent
5 involvement of the central DM, with the development of endothelial decompensation,
6 manifest by corneal epithelial and stromal edema, in some individuals. While the reported
7 clinical features of this pedigree are similar to those of PMED, the authors identified a
8 heterozygous *KIAA1522* (c.1331G>A) variant that segregated with affected status in the
9 pedigree, indicating a distinct genetic basis from the families that we report.²⁶

10 With the elucidation of the genetic basis of essentially all of the corneal dystrophies and the
11 initiation of preclinical trials of gene therapy for selected corneal dystrophies, we propose to
12 reconsider the classification system of the corneal dystrophies, with more emphasis placed
13 on the genetic basis and less on the layer of the cornea that is primarily affected. The first
14 FDA-approved gene therapy, Luxturna®, received approval with a genetic indication labeling
15 "for the treatment of patients with confirmed biallelic *RPE65* mutation-associated retinal
16 dystrophy".²⁷ This wording was selected primarily based on the observed variety of clinical
17 diagnoses for *RPE65*-mediated inherited retinal diseases, despite common characteristic
18 findings such as nyctalopia. Depending on the time of disease onset, severity, rate of
19 progression and presenting phenotype, the most common diagnoses for *RPE65*-mediated
20 inherited retinal diseases include Leber congenital amaurosis (LCA), early-onset severe
21 retinal dystrophy (EOSRD), retinitis pigmentosa (RP), Fundus albipunctatus (FA) and
22 others.^{28,29} However, regardless of the clinical diagnosis, confirmation of biallelic *RPE65*
23 mutations is required for a patient to be eligible for Luxturna® gene therapy. Similarly, as the
24 *TGFB1* epithelial-stromal dystrophies demonstrate significant phenotypic heterogeneity and
25 involve multiple layers of the cornea, they are more accurately classified and conceptualized

2
3 using a molecular genetic rather than an anatomic construct. Given the fact that both MCD
4 and PMED are associated with promoter and coding region mutations in *CHST6*, we propose
5
6 that they should both be categorized as *CHST6*-associated corneal dystrophies. The shifting
7 of the emphasis from variable phenotypic features to the invariant underlying genetic defects
8 associated with the corneal dystrophies is a natural and necessary evolution as we enter the
9 era of genetic therapy for corneal dystrophies.
10
11
12
13
14
15
16
17
18
19
20
21
22
23
24
25
26
27
28
29
30
31
32
33
34
35
36
37
38
39
40
41
42
43
44
45
46
47
48
49
50
51
52
53
54
55
56
57
58
59
60
61
62
63
64
65

4 **AUTHOR CONTRIBUTIONS**564 **Wenlin Zhang:** Conceptualization, Methodology, Formal Analysis, Investigation, Data

565 Curation, Writing-Original Draft, Writing-Review & editing, Visualization, Project

566 Administration. **Huong Duong:** Conceptualization, Validation, Investigation, Data Curation,567 Writing-Review & editing, Supervision, Project Administration. **Passara Jongkhajornpong:**568 Conceptualization, Validation, Investigation, Data Curation, Writing-Review & editing. **Do Thi**569 **Thuy Hang:** Validation, Investigation, Data Curation. **Huan Pham:** Validation, Investigation,570 Data Curation. **Mai Nguyen:** Validation, Investigation, Data Curation. **Charlene Choo:**571 Validation, Investigation, Data Curation. **Dominic Williams:** Investigation, Data Curation572 **Xuan Nguyen:** Investigation, Data Curation. **Tien Dat Nguyen:** Investigation, Data Curation.573 **Brian Aguirre:** Investigation, Data Curation. **Shaukat Khan:** Investigation, Data Curation.574 **Madhuri Wadehra:** Supervision, **Shunji Tomatsu:** Methodology, Writing-Review & editing,575 Supervision, Project Administration. **Anthony J. Aldave:** Conceptualization, Methodology,

576 Writing-Review & editing, Supervision, Project Administration. Funding Acquisition.

4 **ACKNOWLEDGEMENTS/DISCLOSURE**

5
6 Funding: This work was supported by the National Eye Institute P30EY000331 (core grant to
7
8 the Stein Eye Institute), and an unrestricted grant from Research to Prevent Blindness (Stein
9
10 Eye Institute)

11
12 Financial Disclosures: No financial disclosures

13
14 We thank Dr. Tomoya O. Akama (Kansai Medical University) for the generous gifts of
15
16 pcDNA3_CGn6ST, pcDNA3_KSG6ST and pcDNA3_b3GnT7 plasmids, Dr. James V. Jester
17
18 (UC Irvine) for the generous gift of a telomerase immortalized human keratocyte cell line and
19
20 Dr. Ula V. Jurkunas (Massachusetts Eye and Ear) for the generous gift of a telomerase
21
22 immortalized human endothelial cell line.

23

24

25

26

27

28

29

30

31

32

33

34

35

36

37

38

39

40

41

42

43

44

45

46

47

48

49

50

51

52

53

54

55

56

57

58

59

60

61

62

63

64

65

4 REFERENCES

- 5
6
7
8
9
10 Weiss JS, Moller HU, Aldave AJ, et al. IC3D classification of corneal dystrophies--edition 2.
11 Cornea. 2015;34(2):117-159.
- 12 Weiss JS, Rapuano CJ, Seitz B, et al. IC3D Classification of Corneal Dystrophies-Edition 3.
13 Cornea. 2024;43(4):466-527.
- 14 Bendl J, Musil M, Stourac J, Zendulka J, Damborsky J, Brezovsky J. PredictSNP2: A Unified
15 Platform for Accurately Evaluating SNP Effects by Exploiting the Different Characteristics of Variants
16 in Distinct Genomic Regions. *PLoS Comput Biol.* 2016;12(5):e1004962.
- 17 Adzhubei IA, Schmidt S, Peshkin L, et al. A method and server for predicting damaging
18 missense mutations. *Nature methods.* 2010;7(4):248-249.
- 19 Boyle AP, Hong EL, Hariharan M, et al. Annotation of functional variation in personal genomes
20 using RegulomeDB. *Genome Res.* 2012;22(9):1790-1797.
- 21 Abascal F, Acosta R, Addleman NJ, et al. Expanded encyclopaedias of DNA elements in the
22 human and mouse genomes. *Nature.* 2020;583(7818):699-710.
- 23 Zhou J, Theesfeld CL, Yao K, Chen KM, Wong AK, Troyanskaya OG. Deep learning
24 sequence-based ab initio prediction of variant effects on expression and disease risk. *Nature*
25 Genetics. 2018;50(8):1171-1179.
- 26 Consortium EP, Moore JE, Purcaro MJ, et al. Expanded encyclopaedias of DNA elements in
27 the human and mouse genomes. *Nature.* 2020;583(7818):699-710.
- 28 Akama TO, Nakayama J, Nishida K, et al. Human corneal GlcNac 6-O-sulfotransferase and
29 mouse intestinal GlcNac 6-O-sulfotransferase both produce keratan sulfate. *J Biol Chem.*
30 2001;276(19):16271-16278.
- 31 Schmedt T, Chen Y, Nguyen TT, Li S, Bonanno JA, Jurkunas UV. Telomerase immortalization
32 of human corneal endothelial cells yields functional hexagonal monolayers. *PLoS One.*
33 2012;7(12):e51427.

- 2
3 11. Jester JV, Huang J, Fisher S, et al. Myofibroblast differentiation of normal human keratocytes
4 and hTERT, extended-life human corneal fibroblasts. *Invest Ophthalmol Vis Sci.* 2003;44(5):1850-
5 1858.
6
7 12. Tomatsu S, Shimada T, Mason RW, et al. Establishment of glycosaminoglycan assays for
8 mucopolysaccharidoses. *Metabolites.* 2014;4(3):655-679.
9
10 13. Kubaski F, Suzuki Y, Orii K, et al. Glycosaminoglycan levels in dried blood spots of patients
11 with mucopolysaccharidoses and mucolipidoses. *Mol Genet Metab.* 2017;120(3):247-254.
12
13 14. Tavtigian SV, Greenblatt MS, Harrison SM, et al. Modeling the ACMG/AMP variant
14 classification guidelines as a Bayesian classification framework. *Genet Med.* 2018;20(9):1054-1060.
15
16 15. Brnich SE, Rivera-Munoz EA, Berg JS. Quantifying the potential of functional evidence to
17 reclassify variants of uncertain significance in the categorical and Bayesian interpretation frameworks.
18
19 16. Harrison SM, Biesecker LG, Rehm HL. Overview of Specifications to the ACMG/AMP Variant
20 Interpretation Guidelines. *Curr Protoc Hum Genet.* 2019;103(1):e93.
21
22 17. Akama TO, Nishida K, Nakayama J, et al. Macular corneal dystrophy type I and type II are
23 caused by distinct mutations in a new sulphotransferase gene. *Nat Genet.* 2000;26(2):237-241.
24
25 18. Richards S, Aziz N, Bale S, et al. Standards and guidelines for the interpretation of sequence
26 variants: a joint consensus recommendation of the American College of Medical Genetics and
27 Genomics and the Association for Molecular Pathology. *Genet Med.* 2015;17(5):405-424.
28
29 19. Biesecker LG, Harrison SM. The ACMG/AMP reputable source criteria for the interpretation of
30 sequence variants. *Genetics in Medicine.* 2018;20(12):1687-1688.
31
32 20. Brnich SE, Abou Tayoun AN, Couch FJ, et al. Recommendations for application of the
33 functional evidence PS3/BS3 criterion using the ACMG/AMP sequence variant interpretation
34 framework. *Genome Medicine.* 2019;12(1):3.
35
36 21. Ellingford JM, Ahn JW, Bagnall RD, et al. Recommendations for clinical interpretation of
37 variants found in non-coding regions of the genome. *Genome Medicine.* 2022;14(1):73.

- 2
3 638 22. Liu Z, Tian X, Iida N, et al. Mutation analysis of CHST6 gene in Chinese patients with macular
4 corneal dystrophy. *Cornea*. 2010;29(8):883-888.
5
6 639 23. Gruenauer-Kloevekorn C, Braeutigam S, Heinritz W, Froster UG, Duncker GI. Macular corneal
7 dystrophy: mutational spectrum in German patients, novel mutations and therapeutic options. *Graefes
8 Arch Clin Exp Ophthalmol*. 2008;246(10):1441-1447.
9
10 640 24. Chaurasia S, Mishra DK. Atypical presentation of macular corneal dystrophy managed by
11 Descemet stripping endothelial keratoplasty. *Indian J Ophthalmol*. 2019;67(1):118-119.
12
13 641 25. Zhang W, Kassels AC, Barrington A, et al. Macular corneal dystrophy with isolated peripheral
14 Descemet membrane deposits. *Am J Ophthalmol Case Rep*. 2019;16:100571.
15
16 642 26. Ye M, Lu Q, Zhao D, et al. New Endothelial Corneal Dystrophy in a Chinese Family. *Cornea*.
17 2023;42(5):529-535.
18
19 643 27. LUXURNA (voretigene neparvovec-rzyl) intraocular suspension for subretinal injection
20 [package insert]. Philadelphia, PA: Spark Therapeutics, Inc.; 2022.
21
22 644 28. Maguire AM, Bennett J, Aleman EM, Leroy BP, Aleman TS. Clinical Perspective: Treating
23 RPE65-Associated Retinal Dystrophy. *Mol Ther*. 2021;29(2):442-463.
24
25 645 29. Sodi A, Banfi S, Testa F, et al. RPE65-associated inherited retinal diseases: consensus
26 recommendations for eligibility to gene therapy. *Orphanet Journal of Rare Diseases*. 2021;16(1):257.
27
28 646
29
30 647
31
32 648
33
34 649
35
36 650
37
38 651
39
40 652
41
42 653
43
44 654
45
46
47
48
49
50
51
52
53
54
55
56
57
58
59
60
61
62
63
64
65

4 **FIGURE CAPTIONS**

5
6 **Figure 1. Pedigrees of seven previously unreported families with Peripheral macular**
7 **endothelial dystrophy (PMED).** Family A is Thai, families B – G are Vietnamese. The
8 arrowhead indicates the proband in each family. Asterisks indicate enrolled individuals that
9 were examined and had genomic DNA collected. Filled symbols indicate affected individuals,
10 empty symbols indicate unaffected individuals. Question marks (?) indicate individuals who
11 were not examined and are of undetermined affected status. Diagonal lines mark deceased
12 individuals. “WES” indicates individuals in whom whole exome sequencing was performed.
13 Red dot “•” indicates individuals from whom dried blood spots were collected for measurement
14 of sulfated GAGs. Red “drop shape” indicates individuals from whom serum was collected for
15 measurement of sulfated GAGs. “EK” indicates individuals in whom endothelial keratoplasty
16 was performed in at least one eye.

17
18 **Figure 2. Clinical findings of affected individuals in Families A (panels A-C), B (D-G) and**
19 **C (H-J).** (A) Slit lamp photomicrographs of the proband. (B) Slit lamp photomicrographs of the
20 proband following DMEK in both eyes. (C) Slit lamp photomicrographs of the affected mother
21 of the proband. (D) Slit lamp photomicrographs of the proband at initial presentation and (E)
22 six months following presentation. (F) Slit lamp photos of the proband following DSAEK in the
23 right eye. (G) Slit lamp photomicrographs of the proband’s older brother. (H) Slit lamp
24 photomicrographs of the proband at presentation. (I) Slit lamp photomicrographs of the
25 proband’s left eye following DMEK. (J) Slit lamp photos of the proband’s affected older sister.

26
27 **Figure 3. Clinical findings of affected individuals in Families D (panels A-D), E (E-F), F**
28 **(G-H) and G (I).** (A) Slit lamp photomicrographs of the proband at presentation. (B) AS-OCT
29 images of the proband at presentation. (C) Slit lamp photomicrographs of one of the proband’s

2 affected younger brothers. (D) Slit lamp photomicrographs of the other affected younger
3 brother of the proband. (E) Slit lamp photomicrographs of the proband at presentation. (F) Slit
4 lamp photomicrographs of the affected younger sister of the proband. (G) Slit lamp
5 photomicrographs of the proband at presentation. (H) Slit lamp photomicrographs of the
6 proband's left eye following DSEK. (I) Slit lamp photomicrographs of the proband.
7
8
9
10
11
12
13
14
15
16
17
18
19
20
21
22
23
24
25
26
27
28
29
30
31
32
33
34
35
36
37
38
39
40
41
42
43
44
45
46
47
48
49
50
51
52
53
54
55
56
57
58
59
60
61
62
63
64
65

Figure 4. Functional Assay of CHST6 Mutants. (A) Graphical representation of *CHST6* gene structure and map of *CHST6* promoter-containing expressing vector pcDNA3_CGn6STwPro, showing the relative positions of *CHST6* exon 1 – 3 on the genome and in the vector. Color-coded lines depicted the relative positions of generated mutations in the vector. (B) Western Blot results of HCEnC and HK cell lysates following CGn6STwPro transfections. The amount of wild-type (WT) or mutant CGn6STwPro expression vector used was denoted as “2 \times ” for 250 ng / well and “1 \times ” for 125 ng / well. (C) Bar graph summary of 5D4+ KS relative fold change in HCEnC or HK transfected with mutant CGn6STwPro expression vectors when compared to WT/WT transfection.

Figure 5. Histology and immunohistochemistry of DM from three probands. Healthy control cornea: full thickness eye bank donor cornea. PCE DM: DM from an individual with pseudophakic corneal edema.

1 Zhang et al.

2 Peripheral macular endothelial dystrophy

3 1

4 **Peripheral Macular Endothelial Dystrophy: Clinical, Histopathologic, Genetic and**
5
6 **Functional Characterization**

7
8 3 Short title: Peripheral Macular Endothelial Dystrophy

10 12 4 Wenlin Zhang, M.D., Ph.D.,^a Huong Duong, M.D.,^b Passara Jongkajornpong, M.D., Ph.D.,^c

11 14 5 Do Thi Thuy Hang, M.D.,^d Huan Pham, M.D.,^b Mai Nguyen, M.D.,^b Charlene Choo, M.D.,^a

12 17 6 Dominic Williams, M.D.,^a Xuan Nguyen, M.D.,^e Tien Dat Nguyen, M.D.,^e Brian Aguirre,^f

13 19 7 Shaukat Khan, Ph.D.,^g Madhuri Wadehra, Ph.D.,^f Shunji Tomatsu, M.D., Ph.D.,^g and Anthony

21 22 8 J. Aldave, M.D.^{a#}

23 24 9 ^a Stein Eye Institute, UCLA, Los Angeles CA.

25 26 10 ^b Ho Chi Minh City Eye Hospital, Ho Chi Minh City, Vietnam.

27 29 11 ^c Department of Ophthalmology, Faculty of Medicine Ramathibodi Hospital, Mahidol

30 31 12 University, Bangkok, Thailand

32 34 13 ^d Vietnam National Eye Hospital, Hanoi, Vietnam.

33 36 14 ^e University of Medicine and Pharmacy at Ho Chi Minh City, Ho Chi Minh City, Vietnam.

34 39 15 ^f Department of Pathology and Laboratory Medicine, UCLA, Los Angeles, CA.

40 41 16 ^g Nemours Children's Health, Wilmington, DE.

42 43 44 17 Supplemental Material available at AJO.com

45 46 47 48 18 **#Correspondence**

49 50 51 19 Anthony J. Aldave, M.D.

52 53 20 Stein Eye Institute, David Geffen School of Medicine at UCLA, 200 Stein Plaza, UCLA, Los

54 55 21 Angeles, CA 90095-7003

56 57 22 Tel: 310-206-7202

58 59 23 aldave@jsei.ucla.edu

KEYWORDSCorneal endothelial dystrophy, *CHST6*, keratan sulfate

4 26 INTRODUCTION
5
6

7 The corneal dystrophies are a group of inherited disorders that are typically bilateral,
8 symmetric, slowly progressive and are not influenced by environmental or systemic factors¹.
9
10 Traditionally, corneal dystrophies have been anatomically classified, based on the layer of the
11 cornea that is primarily affected: epithelium, Bowman layer, stroma and endothelium.
12
13 However, the International Committee for the Classification of the Corneal Dystrophies has
14 reclassified the dystrophies according to the cellular origin of the dystrophic deposits, and
15 thus the *TGFB1* dystrophies are now classified as epithelial-stromal dystrophies.² In the case
16 of macular corneal dystrophy (MCD), although histopathologic examination demonstrates
17 non-sulfated/low-sulfated glycosaminoglycans (GAG) in both the stroma and the
18 endothelium, it remains classified as a stromal dystrophy due to the presence of macular
19 stromal deposits and diffuse stromal haze that characterize MCD and the absence of
20 evidence of endothelial dysfunction in affected individuals.

21
22
23 MCD is associated with mutations in the *CHST6* gene, encoding corneal N-
24 acetylglucosamine-6-O-sulfotransferase (CGn6ST or GlcNAc6ST), which plays an essential
25 role in the sulfation of GAG in the cornea by catalyzing the transfer of sulfate from 3'-
26 phosphoadenosine 5'-phosphosulfate to position 6 of a non-reducing N-acetylglucosamine
27 (GlcNAc) residue in keratan sulfate (KS). Decreased CGn6ST/GlcNAc6ST activity in the
28 corneal keratocytes in individuals with MCD leads to the accumulation of Alcian blue-positive
29 non-sulfated/low-sulfated GAG deposits (decreased sulfation of KS) within keratocytes and in
30 the extracellular corneal stroma, resulting in loss of corneal clarity.

31
32 In the current study, we describe a corneal endothelial dystrophy that is characterized by
33 peripheral posterior corneal macular opacities reminiscent of those associated with MCD, but
34 without the macular stromal deposits and diffuse stromal haze that are essential phenotypic

2 features of MCD. Given this, the development of corneal edema in symptomatic individuals
3 and the successful restoration of vision with endothelial keratoplasty as well as the functional
4 impact of the associated *CHST6* promoter mutation, we propose the classification of this
5 dystrophy, which we have named Peripheral macular endothelial dystrophy (PMED), and
6 MCD as *CHST6*-associated corneal dystrophies.

7
8
9
10
11
12
13
14

15
16
17
18
19
20
21
22
23
24

25
26
27
28
29
30
31
32
33
34

35
36
37
38
39

40
41
42
43
44

45
46
47

48
49
50

51
52
53
54

55
56
57

58
59
60

61
62
63
64
65

MATERIALS AND METHODS

Approval for this *observational case seriesstudy* was obtained from the Institutional Review Board at the University of California at Los Angeles (UCLA IRB#11–000020). Written informed consent was obtained from all subjects in this study according to the tenets of the Declaration of Helsinki.

Clinical Evaluation

All affected and unaffected individuals from seven families who agreed to participate in the study underwent a comprehensive ophthalmic examination (Fig. 1), including slit lamp biomicroscopy and photography, ultrasound biomicroscopy (UBM), Scheimpflug imaging (Oculus Pentacam), and anterior segment optical coherence tomography (AS-OCT). The diagnosis of PMED was established based on the presence of round, gray-white, discrete deposits confined to the peripheral Descemet membrane (DM) or posterior surface of the cornea, without stromal opacities or haze and with or without corneal epithelial and/or stromal edema.

Sanger Sequencing of CHST6

After obtaining informed consent, saliva and/or blood samples were collected from members of each of the seven families using a saliva collection kit (Oragene, DNA Genotek, Inc.) or a standard phlebotomy procedure. Genomic DNA was isolated from saliva samples using the Oragene Purifier (OG-L2P, DNA Genotek, Inc.) and from blood samples using the FlexiGene DNA Kit (QIAGEN), according to the manufacturer's instructions. Each of the three exons of *CHST6* and the 2.5 kb region upstream of exon 1 were amplified by PCR and sequenced using Sanger sequencing (Supplemental Materials, Primers and PCR conditions used for *CHST6* screening) (Supplemental Table 1). Sequences were compared to the wild-type

2
3
4 CHST6 gene transcript (NM_021615), and the minor allele frequencies (MAF) of identified
5 variants were obtained from public databases including Exome Aggregation Consortium
6 (ExAC), 1000 Genomes Project (1000Genome), Trans-Omics for Precision Medicine
7 (TOPMED) and Genome Aggregation Database (gnomAD). A rare variant was defined as a
8 variant with MAF < 0.01 in all databases.
9
10
11
12
13
14
15
16
17
18

19 *Whole Exome Sequencing (WES) and Data Analysis*

20 WES was performed on the genomic DNA of all enrolled members from PMED families A, B,
21 and C (Fig. 1). DNA libraries were prepared using the TruSeq DNA Sample Preparation Kit
22 v2 (Illumina Inc.), and exome capture was performed with the SeqCap EZ Exome Library
23 v2 (Roche NimbleGen, Inc.). Paired-end sequencing (2×150 bp) was carried out on
24 Illumina's HiSeq 3000 platform. The generated raw sequence reads were aligned to Genome
25 Research Consortium human build 38 (GRCh38) using Burrows-Wheeler Aligner (BWA) in
26 maximal exact match (MEM) mode and subsequently processed following the Genome
27 Analysis Toolkit (GATK) best practice guidelines for variant calling (Supplemental Materials,
28 GATK variant calling). After variant calling, common variants (MAF > 0.01) were filtered out,
29 and rare variants were annotated using the Ensembl Variant Effect Predictor (VEP) online
30 tool. Coding non-synonymous variants and splice site variants were retained and analyzed
31 for segregation with the affected status in Family C using both autosomal recessive and
32 autosomal dominant models, and genes containing potentially pathogenic variants were
33 subsequently screened in members of Families B and C (Supplemental Materials, WES
34 variant filtration).

35 *In silico variant prediction and scoring*

36 The identified CHST6 coding variants were analyzed using the online tools PredictSNP2 and

2
3 PolyPhen-2 to assess their potential impact on protein function.^{3,4} PredictSNP2 is a
4 consensus classifier that combines five prediction methods, including Combined Annotation
5
6 Dependent Depletion (CADD), Deleterious Annotation of Genetic Variants using Neural
7 Networks (DANN), Functional Analysis through Hidden Markov Models (FATHMM), FunSeq2
8 and Genome Wide Annotation of Variants (GWAVA).³ The identified *CHST6* promoter
9 variants were analyzed using the online tool RegulomeDB to determine the likelihood of each
10 variant being in a regulatory region bound by subunits of transcriptional machinery and/or
11 transcriptional factors.⁵ The RegulomeDB score represents a model that integrates functional
12 genomics features, including continuous values from multiple databases such as chromatin
13 immunoprecipitation sequencing (ChIP-seq) signal and DNase-seq signal from The
14 Encyclopedia of DNA Elements (ENCODE), information content change, and predicted
15 scores from the deep learning sequence-based algorithmic program DeepSEA.^{6,7}

16 *In vitro CHST6 functional assay*

17 For the functional assay, we generated a *CHST6* expression vector containing the native
18 promoter of *CHST6*. Briefly, a 1439 bp fragment encompassing exon 1 of the *CHST6* gene,
19 the predicted *CHST6* promoter and two adjacent enhancers (identified based on ENCODE
20 registry of candidate cis-regulatory elements (cCREs)), was cloned into the previously
21 described *CHST6* expression vector pcDNA3-CGn6ST.^{8,9} The cloning replaced the
22 sequences of CMV enhancer-containing promoter and T7 promoter. The pcDNA3-CGn6ST
23 vector contains the nucleotide sequences of exons 2 and 3 of the *CHST6* gene. The newly
24 cloned *CHST6* native promoter-containing *CHST6* expression vector was named pcDNA3-
25 CGn6STwPro and contained the wild-type sequences of the non-coding 5' region, the non-
26 coding exons 1 and 2, and the entire coding sequence of exon 3 of the *CHST6* gene. Site-
27 directed mutagenesis was then performed on pcDNA3-CGn6STwPro, also denoted as
28
29
30
31
32
33
34
35
36
37
38
39
40
41
42
43
44
45
46
47
48
49
50
51
52
53
54
55
56
57
58
59
60
61
62
63
64
65

2 CGn6STwPro_WT, to generate nucleotide changes consistent with the mutations found in
3 PMED pedigrees (QuikChange Lightning Site-Directed Mutagenesis Kit, Agilent
4 Technologies). The following three single mutant constructs were created: CGn6STwPro_c.-
5 690G>C, CGn6STwPro_Y268C (nucleotide change c.803A>G), and CGn6STwPro_P280L
6 (nucleotide change c.839C>T). Additionally, exon 1 of the *CHST6* gene along with
7 surrounding sequences (1439 bp) from the proband of family B was cloned into pcDNA3-
8 CGn6ST using the same method as described above. This generated pcDNA3-
9 CGn6STwPro_PT, which contained three adjacent variants (c.[-668C>T; -690G>C; -
10 792C>T]). All mutations were confirmed by Sanger sequencing (Laragen, Inc., Culver City,
11 CA).

12 To investigate the functional impact of the identified *CHST6* mutations in human

13 corneal endothelial cells and keratocytes, telomerase immortalized human corneal
14 endothelial cells (HCEnC) and keratocytes (HK) were transfected with wild-type and/or
15 mutant CHST6 promoter-containing expressing vectors (CGn6STwPro) using
16 Lipofectamine® LTX with PLUS reagent (A12621, Life Technologies) according to the
17 manufacturer's recommendations (Supplemental Materials, Human corneal endothelial cell
18 line cell culture, Human corneal keratocyte cell culture).^{10,11} To enhance the detection of
19 sulfated KS, HCEnC or HK (seeded in 24-well plates at 50% confluence 24 hours prior) were
20 co-transfected with expression vectors b3GnT7 (250 ng/well) and HKSG6ST (250 ng/well),
21 two enzymes involved in the extension of KS and C-6 sulfation of Gal residue in KS, along
22 with CGn6STwPro wild-type and/or mutant (250 ng/well). To simulate compound
23 heterozygous *CHST6* mutations identified in some affected individuals, an equal amount of
24 two CGn6STwPro mutant constructs (125 ng/well) were used. A total of 750 ng of plasmid
25 DNA was used per well.

149 The following combination of CGn6STwPro constructs were used to mimic the *CHST6*
150 mutation status observed in individuals reported here: 1) WT/WT, representing the healthy
151 control without *CHST6* mutations; 2) PT/PT, representing affected individuals with
152 homozygous variant c.[-668C>T; -690G>C; -792C>T] in Families B, E, and G; 3) PT/P280L,
153 mimicking the proband of Family A with compound heterozygous variants c.[-668C>T; -
154 690G>C; -792C>T] and the previously unreported P280L; 4) PT/Y268C, mimicking the
155 affected individuals in Family C with compound heterozygous variants c.[-668C>T; -690G>C;
156 -792C>T] and Y268C; 5) WT/PT, mimicking the affected mother of the proband (I-2) in Family
157 A with heterozygous variant c.[-668C>T; -690G>C; -792C>T]; 6) c.-690G>C/c.-690G>C
158 (CGn6STwPro_c.-690G>C), assessing the impact of isolated homozygous variant c.-690G>C
159 without two adjacent variants c.-668C>T and c.-792C>T; 7) c.-690G>C/P280L, assessing the
160 impact of compound heterozygous variants c.-690G>C and P280L; 8) c.-690G>C/Y268C,
161 assessing the impact of compound heterozygous variants c.-690G>C and Y268C; 9)
162 P280L/P280L (CGn6STwPro_P280L), assessing the impact of homozygous variant P280L;
163 and 10) Y268C/Y268C (CGn6STwPro_Y268C), assessing the impact of homozygous variant
164 Y268C on CGn6ST/CHST6 enzymatic function.

165 The enzymatic activities of CGn6ST, together with b3GnT7 and HKSG6ST, result in
166 highly sulfated KS, which can be detected by the 5D4 antibody (MABN2483, Millipore
167 Sigma). Forty-eight hours post-transfection, cells were lysed with radioimmunoprecipitation
168 assay (RIPA) buffer containing proteinase and phosphatase inhibitors. Total protein was
169 quantified using the bicinchoninic acid (BCA) assay, separated and detected using a
170 capillary-based Western Blot system (Simple Western assay Wes, ProteinSimple). Highly
171 sulfated KS, b3GnT7 protein and GAPDH were detected using 5D4, anti-B3GNT7 (NBP1-
172 69637, Novus Biological) and anti-GAPDH (MAB374, Millipore Sigma) antibodies,

2
3 respectively. Quantification and data analysis were performed using the Compass for Simple
4 Western software (ProteinSimple). The level of 5D4-positive sulfated KS was normalized to
5 GAPDH as the loading control and then to B3GNT7 as an internal control for transfection
6 efficiency in each sample. Four biological replicates of transfection and Western Blot were
7 performed, and the average 5D4+ KS level was calculated for each CHST6 mutant or
8 combination of mutants.

9 *Histology and Immunofluorescence Staining*

10 Five-micrometer sections of paraffin-embedded corneas from seven healthy donors, surgical
11 DM specimens from three probands from families A, C, and F, and a surgical DM specimen
12 from an individual with pseudophakic corneal edema (PCE) were deparaffinized and
13 rehydrated in a graded ethanol series (100%, 95%, 70% and 50%).

14 H&E staining of specimens was performed following a standardized protocol
15 (Translational Pathology Core Laboratory, Department of Pathology, UCLA). For Alcian blue
16 staining, the rehydrated sections were stained with an Alcian blue solution (1% Alcian blue in
17 3% acetic acid in deionized water; pH = 2.5) for 30 minutes, followed by staining with a 0.5%
18 aqueous neutral red solution for 2 minutes. For high iron diamine staining, the rehydrated
19 sections were stained with a high iron diamine solution (0.24% N, N-dimethyl-meta-
20 phenylenediamine dihydrochloride, 0.04% N, N-dimethyl-para-phenylenediamine
21 dihydrochloride, 2.8% Ferric Chloride in deionized water) for 18 hours, followed by staining
22 with a 0.5% aqueous neutral red solution for 2 minutes. H&E, Alcian Blue or high iron diamine
23 stained sections were imaged with a KEYENCE BZ-X700 all-in-one fluorescence microscope.

24
25 For 5D4 staining, the rehydrated sections underwent antigen retrieval in 10 mM sodium
26 citrate, followed by a standard immunofluorescence staining protocol with the 5D4 antibody

2 overnight at 4°C and Alexa 568 anti-mouse secondary antibody with DAPI. For Lectin-FITC
3 staining, the rehydrated sections underwent antigen retrieval in a citrate-based antigen
4 unmasking solution (Vector Labs, #H-3300) for 25 minutes, followed by a standard
5 immunofluorescence staining protocol with Lectin-FITC conjugated antibody (Vector
6 Laboratories, #FL-1171). 5D4 and Lectin-FITC stained sections were imaged with an inverted
7 confocal fluorescence microscope (Olympus FV-1000, Olympus Corporation).

8 *Sulfated Glycosaminoglycan Measurement in Serum and/or Dried Blood Spots*

9 The sulfation levels of serum GAG, including dermatan sulfate (DS), heparan sulfate (HS),
10 and KS, were measured by liquid chromatography with tandem mass spectrometry (LC-
11 MS/MS) as previously described and the results were compared with age-matched
12 controls.^{12,13} Serum samples were collected from 17 individuals and dried blot spots (DBS)
13 were collected from 10 individuals from the seven families (Fig. 1).

14 *Calculation of Odds of Pathogenicity (Odds Path) for Identified Variants*

15 The number of criteria met for each identified *CHST6* variant was counted as N for each
16 criterion subtype, including benign supporting (BP1–6), benign strong (BS1–4), benign stand-
17 alone (BA1), pathogenic supporting (PP1–5), pathogenic moderate (PM1–6), pathogenic
18 strong (PS1–4), or very strong (PVS1). The odds of pathogenicity (*OddsPath*) of each variant
19 was calculated using the following published formula *OddsPath* =

$$20 \quad 350 \left(\frac{N_{PP}}{8} + \frac{N_{PM}}{4} + \frac{N_{PS}}{2} + \frac{N_{PVS}}{1} - \frac{N_{BP}}{8} - \frac{N_{BS}}{2} \right)^{14}$$

21 The Bayesian posterior probability was calculated by the
22 equation $Post_P = \frac{OddsPath * Prior_P}{(OddsPath - 1) * Prior_P + 1}$, in which prior probability (*Prior_P*) by default is 0.1.

23 *Post_P* was then assigned a variant classification as follows: benign < 0.001; 0.001 ≤ likely
24 benign < 0.1; 0.1 ≤ Variant of Uncertain Significance (VUS) < 0.90; 0.90 ≤ likely pathogenic <

3 18 0.99; 0.99 ≤ pathogenic.¹⁵ OddsPath cut-off scores for Supporting, Moderate, Strong, and
4 19 Very Strong pathogenic evidence were obtained from published guidelines.¹⁶
5
6
7
8
9
10
11
12
13
14
15
16
17
18
19
20
21
22
23
24
25
26
27
28
29
30
31
32
33
34
35
36
37
38
39
40
41
42
43
44
45
46
47
48
49
50
51
52
53
54
55
56
57
58
59
60
61
62
63
64
65

4 **RESULTS**5 **Clinical Features**6 *7 Family A*

8
9 A 47-year-old Thai woman (Fig. 1. A. II-2) with an unremarkable past medical history
10 presented with progressive decrease in vision in both eyes. Corrected visual acuities (CVA)
11 measured 20/40 OD and 20/50 OS. Slit lamp biomicroscopy and AS-OCT revealed inferior
12 paracentral corneal subepithelial fibrosis, underlying stromal edema and multiple discrete
13 gray peripheral opacities at the level of DM, predominantly located in the superior and inferior
14 peripheral cornea (Fig. 2A, Supplemental Fig. 1A). Central corneal pachymetry measured
15 626 µm OD and 604 µm OS. A combined Descemet membrane endothelial keratoplasty
16 (DMEK), cataract extraction was performed in each eye with restoration of stromal clarity
17 other than for residual inferior paracentral subepithelial scarring (Fig. 2B). Slit lamp
18 examination of other family members revealed similar appearing discrete gray opacities only
19 in the proband's 73-year-old mother, whose CVA measured 20/70 OU (Fig. 1. A. I-2). As the
20 opacities in proband's mother were confined to the inferior peripheral cornea in each eye,
21 were significantly fewer in number, and were not associated with corneal edema (Fig. 2C),
22 her decreased corrected visual acuity was attributed to bilateral severe nuclear sclerosis. The
23 other examined family members, including the proband's father (Fig. 1. A. I-1), older sister
24 (Fig. 1. A. II-1), and daughter (Fig. 1. A. III-1), demonstrated clear corneas.
25
26

27 *Family B*

28 A 49-year-old Vietnamese woman (Fig. 1. B. II-1) with an unremarkable past medical history
29 presented with glare, halo, and foreign body sensation in both eyes (OD > OS) that was
30 worse in the morning. Slit lamp biomicroscopy revealed mild diffuse corneal stromal edema
31
32

2
3
4 OD and trace stromal edema OS with multiple discrete grayish peripheral opacities at the
5 level of DM in both eyes (Fig. 2D). The patient complained of progressive loss of vision
6 thereafter for 6 months as CVA declined from 20/100 to counting finger (CF) at 2 meters OD
7 and from 20/20 to 20/25 OS. Slit lamp biomicroscopy revealed temporal microcystic epithelial
8 and stromal edema extending to the central cornea in both eyes (Fig. 2E). Central corneal
9 pachymetry measured by UBM was 620 μm OU. A combined Descemet stripping automated
10 endothelial keratoplasty (DSAEK), cataract extraction was performed in the right eye, and the
11 central cornea remained clear 2 years (Fig. 2F) and 4 years later with CVA of 20/25 and
12 20/30, respectively. The unoperated left eye developed progressive subepithelial scarring
13 and stromal edema with CVA decreasing to CF at 3 meters.
14
15
16
17
18
19
20
21
22
23
24
25
26
27
28
29
30
31
32
33
34
35
36
37
38
39
40
41
42
43
44
45
46
47
48
49
50
51
52
53
54
55
56
57
58
59
60
61
62
63
64
65

The parents of the proband (Fig. 1. B. I-1 and B. I-2), who are first cousins, were not available for examination. The proband's younger brother (Fig. 1. B. II-2), who was diagnosed with Fuchs endothelial corneal dystrophy and progressive moderate glaucoma, underwent two DSAEK procedures and tube shunt placement twice in the left eye. Postoperative CVA in the left eye was limited to hand motion due to glaucomatous optic neuropathy. In the unoperated right eye, CVA measured 20/30. Trace peripheral corneal stromal edema and a few peripheral grey macular deposits at the level of DM were observed (Fig. 2G), with central and peripheral corneal pachymetry measuring 570 μm and 830-970 μm , respectively.
Examination of the proband's son (Fig. 1. B. III-1) revealed a clear cornea in each eye.

Family C

A 60-year-old Vietnamese man (Fig. 1. C. II-5) presented with decreased vision in the left eye. Slit lamp examination revealed fine peripheral gray-white opacities at the level of the DM and central guttae in the right eye, and fine central epithelial edema, moderate stromal

2 edema and DM folds in the left eye (Fig. 2H). CVA measured 20/70 OD and CF at 1 meter
3 OS, while central pachymetry measured 457 µm OD and 602 µm OS. A combined DMEK,
4 cataract extraction was performed in the left eye, with the restoration of a clear cornea (Fig.
5 2I). Examination of the proband's 72-year-old sister (Fig. 1. C. II-1) revealed similar
6 appearing white macular deposits, more profound in size and number, primarily located in the
7 superior and inferior posterior peripheral cornea in both eyes (Fig. 2J). Trace corneal stromal
8 edema was present in both eyes with central corneal pachymetry measuring 551 µm OD and
9 532 µm OS. Eight other family members who were examined demonstrated clear corneas
10 (Fig. 1. C). The parents of the proband, who were third cousins, were deceased and their
11 medical records were not available.

12
13
14
15
16
17
18
19
20
21
22
23
24
25
26
27
28
29
30
31
32
33
34
35
36
37
38
39
40
41
42
43
44
45
46
47
48
49
50
51
52
53
54
55
56
57
58
59
60
61
62
63
64
65

Family D

32 A 41-year-old Vietnamese man (Fig. 1. D. II-1) presented with blurred vision and foreign body
33 sensation, worse in the morning, in both eyes (OS > OD) for two years. Corrected visual
34 acuity measured 20/25 OD and 20/50 OS. Slit lamp biomicroscopy revealed moderate diffuse
35 stromal edema, 3+ endothelial guttae and peripheral grey-white discrete opacities at the level
36 of the DM in both eyes (Fig. 3A). Central corneal pachymetry measured by Pentacam for the
37 central 0-2 mm zone was 505 – 522 µm OD and 545 - 742 µm OS and AS-OCT revealed
38 stromal edema and DM folds in the left eye (Fig. 3B). Examination of the proband's 36-year-
39 old brother (Fig. 1. D. II-3) revealed no stromal edema, central 2 mm guttae, and a few fine
40 opacities in the peripheral superior posterior cornea of the right eye. His left eye
41 demonstrated focal inferior paracentral corneal epithelial and stromal edema, and a few
42 discrete grey macular opacites at the level of DM in the superior and nasal periphery (Fig.
43 3C). Examination of the proband's 31-year-old brother (Fig. 1. D. II-5) revealed a few discrete
44

4 gray posterior stromal opacities bilaterally, located only in superior peripheral cornea, without
5 corneal edema (Fig. 3D). Eight other family members who were examined demonstrated
6 clear corneas (Fig. 1. D).

7

8 *Family E*

9

10 A 54-year-old Vietnamese woman (Fig. 1. E. II-1) presented with a progressive decrease in
11 vision and foreign body sensation in both eyes for four years. CVA measured CF at 0.2 meter
12 OD and at 0.5 meter OS. Slit lamp examination revealed central corneal epithelial bullae,
13 diffuse moderate stromal edema, and fine peripheral grey macular deposits at the level of
14 DM, primarily in the superior and inferior peripheral cornea, in both eyes (Fig. 3E). AS-OCT
15 imaging revealed corneal epithelial and stromal edema in both eyes, and central corneal
16 thickness measured 685 – 696 µm OD and 715 µm OS using AS-OCT (Supplemental Fig.
17 31)

18 1B). The proband's 42-year-old younger sister (Fig. 1. E. II-2) had CVA of CF at 0.2 meters
19 OD and CF at 0.6 meters OS secondary to epithelial bullae, subepithelial fibrosis and stromal
20 edema in both eyes (Fig. 3F). Central corneal pachymetry measured 851 µm OD and 836 µm
21 OS using AS-OCT (Supplemental Fig. 1C).

22

23 *Family F*

24

25 A 64-year-old Vietnamese man (Fig. 1. F. I-1) presented with a two-year history of declining
26 vision in both eyes, with CVA decreasing from 20/40 to 20/100 in the right eye and from
27 20/100 to hand motion in the left eye. Slit lamp biomicroscopy revealed fine grey-white
28 peripheral opacities at the level of the DM in both eyes (Fig. 3G). Focal inferior epithelial and
29 diffuse mild stromal edema were present in the right cornea, while diffuse epithelial edema,
30 subepithelial fibrosis and severe stromal edema were present in the left eye. Central corneal
31 pachymetry measured 700 µm OD and 1100 µm OS using UBM. DSEK was performed in the
32

2
3 left eye, after which the corneal edema improved to trace stromal edema and CVA improved
4
5 to counting finger at 1 meter (Fig. 3H).
6
7

8
9 **314 Family G**
10
11

12
13 A 58-year-old Vietnamese man (Fig. 1. G. I-1) presented for evaluation of white deposits in
14 both corneas diagnosed 7 years prior. CVA measured 20/20 OD and 20/25 OS. Slit lamp
15 examination revealed grey-white macular deposits at the level of the DM in both eyes. While
16 the deposits in the paracentral cornea were discrete, they coalesced into confluent opacities
17 on the peripheral posterior cornea of each eye (Fig. 3I).
18
19

20 **320 Genetic Analysis**
21
22

23
24 Identified CHST6 promoter mutation c.-690G>C, in homozygous state or in compound
25 heterozygous state with a coding region mutation, segregated with affected status in seven
26 families
27
28

29
30 The macular appearance of the peripheral opacities in affected individuals prompted
31 screening of the coding and putative promoter regions of the CHST6 gene. A rare promoter
32 mutation n.-97G>C, c.-690G>C (GRCh38.p14 chr16: g.75495538C>G, rs1009794816,
33 GnomAD MAF 0.000064), was identified in all affected individuals in either a homozygous
34 state or in a compound heterozygous state with a CHST6 coding mutation, with the exception
35 of the affected mother of the proband in Family A (Fig. 1. A. I-2) (Table 1). This individual,
36 who displayed a milder corneal phenotype with few deposits and no corneal edema, was
37 heterozygous for the c.-690G>C mutation without a coding region mutation. The affected
38 proband in Family A was compound heterozygous for c.-690G>C and a novel coding region
39 mutation c.839C>T, p.(Pro280Leu) (GRCh38.p14 chr16: g.75478990G>A, rs201767298, no
40
41
42
43
44
45
46
47
48
49
50
51
52
53
54
55
56
57
58
59
60
61
62
63
64
65

2
3 MAF) while unaffected individuals were heterozygous for either mutation. In Family B, E, and
4 G, affected individuals were homozygous and unaffected individuals were heterozygous for
5
6 the c.-690G>C mutation. In Family C, affected individuals were compound heterozygous for
7
8 c.-690G>C with a rare coding mutation c.803A>G, p.(Tyr268Cys) (GRCh38.p14 chr16:
9 g.75479026T>C, rs72547539, GnomAD MAF 0.000064), whereas unaffected individuals
10
11 were heterozygous for one of the two mutations. In Families D and F, affected individuals
12
13 were compound heterozygous for c.-690G>C with a rare coding mutation c.632G>A,
14
15 p.(Arg211Gln) (GRCh38.p14 chr16: g.75479197C>T, rs771397083, GnomAD MAF
16
17 0.000004), while unaffected individuals were heterozygous for one of the two mutations.
18
19

20 Two common promoter variants adjacent to c.-690G>C mutation, c.-792C>T
21
22 (GRCh38.p14 chr16: g.75495640G>A, rs2550322, TOPMED MAF 0.034) and c.-668C>T
23
24 (GRCh38.p14 chr16: g.75495516G>A, rs2550323, TOPMED MAF 0.114) were identified in
25
26 all individuals with the c.-690G>C mutation and were confirmed to be on the same allele (*in*
27
28 *cis*) as c.-690G>C. The three adjacent variants *in cis* are denoted as c.[-668C>T; -690G>C; -
29
30 792C>T]. In regards to the large deletion and rearrangement of *CHST6* upstream region
31
32 previously associated with MCD type II¹⁷, a heterozygous deletion was identified in only one
33
34 of the probands, in family A (Fig. 1. A. II-2).
35
36

37
38 **451 Whole Exome Sequencing fails to identify other candidate genes associated with PMED**
39
40

41 All enrolled individuals from Families A, B, and C underwent WES. Assuming an
42
43 autosomal recessive inheritance in Family C, homozygous or compound heterozygous
44
45 candidate variants that segregated with affected status in Family C were identified in *SND1*,
46
47 *ANKRD36* and *TAS2R43*. However, no candidate variant within these genes segregated with
48
49 the affected status in Families A and B (Supplemental Table 2). Assuming an autosomal
50
51

2
3 dominant inheritance in Family C, heterozygous candidate variants that segregated with
4 affected status in Family C were identified in *CFAP74*, *FAAP20*, *PRDM16*, *CHD5*, *GRB14*,
5
6
7
8 *NUP210*, *ZNF860*, *FAM160A1*, *FAM186A*, *PDIA3* and *NCOA6*. However, no candidate
9 variant within these genes segregated with the affected status in Families A and B, excluding
10 mutations in these genes as the genetic basis of PMED in each of these families
11
12
13 (Supplemental Table 3).
14
15
16

17
18
19 *CHST6 promoter variant c.-690G>C is predicted to be a regulatory variant bound by RNA*
20
21 *polymerase II*
22
23
24

25 *In silico* analysis using RegulomeDB predicted that c.-690G>C is a regulatory variant with a
26 score of 1 on a scale of 0 to 1 (Table 2). This prediction is based on experimental data
27 deposited in the ENCODE database, which includes information on transcriptional factor (TF)
28 binding peaks, DNase footprint, DNase peaks, and the presence of TF binding motif
29 (consensus genomic sequences that specifically bind TF). Among the available ChIP-seq
30 data, the most frequently bound TF or subunit of transcriptional machinery at the genome
31 coordinate of c.-690G>C was RNA polymerase II subunit A (POL2A), observed in 10 out of
32 36 data sets. POL2A is the largest subunit of RNA polymerase II, responsible for synthesizing
33 messenger RNA in eukaryotes. The identified common variants c.-792C>T and c.-668C>T
34 were predicted to be moderately likely regulatory variants with scores of 0.61 and 0.56,
35 respectively (Table 2). *In silico* analysis of the three identified coding variants, p.Arg211Gln,
36 p.Tyr268Cys and p.Pro280Leu, predicted all to be “Deleterious” in PredictSNP2 and
37 “Probably Damaging” in PolyPhen-2 (Table 2).
38
39
40
41
42
43
44
45
46
47
48
49
50
51
52
53
54
55
56
57
58
59
60
61
62
63
64
65

60 *CHST6 c.-690G>C leads to increased sulfated KS in human corneal endothelial cells but not*
61 *in human keratocytes*

2
3
4 To assess the functional effects of the identified *CHST6* variants, wild-type and/or mutant
5
6 *CHST6* promoter-containing expressing vectors (CGn6STwPro) were transfected into
7 immortalized HCEnC and HK (Fig. 4A). In HCEnC, Western Blot results showed low levels of
8
9 5D4+ KS in cells transfected with wild-type *CHST6* expression construct (WT/WT). However,
10
11 increased levels of 5D4+ KS were observed following transfection with either c.-690G>C
12
13 promoter variant-containing construct (PT/PT or c.-690G>C/c.-690G>C), regardless of dose.
14
15
16 The increase in 5D4+ KS was evident in HCEnC transfected under all conditions with c.-
17
18 690G>C promoter variant, including PT/PT, c.-690G>C/c.-690G>C, PT/P280L, PT/Y268C,
19
20
21 WT/PT, c.-690G>C/P280L, or c.-690G>C/Y268C conditions. However, the levels of 5D4+ KS
22
23 remained unchanged in HCEnC following transfection of only coding variant-containing
24
25 constructs P280L/P280L and Y268C/Y268C (Fig. 4B, C).

26
27
28 In HK, on the contrary, there was significantly higher 5D4+ KS in cells transfected with
29 wild-type *CHST6* expression construct (WT/WT) compared to HCEnC WT/WT transfection.
30
31
32 There was no change in 5D4+ KS level following transfection with c.-690G>C promoter
33
34 variant-containing constructs under PT/PT, c.-690G>C/c.-690G>C, PT/P280L, PT/Y268C,
35
36 and WT/PT conditions, compared to HK transfected with WT/WT. Transfection in HK with
37
38 coding variant-containing constructs, including c.-690G>C/P280L, c.-690G>C/Y268C,
39
40 P280L/P280L, and Y268C/Y268C conditions, led to decreased 5D4+ KS levels compared to
41
42 HK transfected with WT/WT. The above data suggested an aberrant 5D4+ KS
43
44 overexpression in HCEnC is induced by the presence of *CHST6* c.-690G>C promoter variant,
45
46 and the previously unreported *CHST6* P280L mutation leads to decreased CGn6ST/*CHST6*
47
48 enzymatic activity in HK, similar to the previously reported Y268C mutation (Fig. 4B, C).

49
50
51
52
53
54
55
56
57
58
59
60
61 *CHST6* c.-690G>C induced increase of sulfated and unsulfated KS is restricted to Descemet
62 membrane and corneal endothelium

2 To investigate whether the aberrant overexpression of 5D4+ KS was the cause of corneal
3 endothelial changes observed in affected individuals in our case series, we performed
4 immunohistochemical staining of three DM samples collected during DMEK surgery of
5 probands of Families A, C and F. A full thickness donor cornea and a DM sample from an
6 individual with pseudophakic corneal edema (PCE) were included as controls. Staining
7 performed included H&E staining, immunofluorescence staining with 5D4 antibody for highly
8 sulfated KS, FITC conjugated Lectin (Lectin-FITC) for non-sulfated KS, Alcian Blue staining
9 for non-sulfated KS and High Iron Diamine (HID) staining for low sulfated KS (Fig. 5). On
10 H&E staining, the DM samples from the three probands showed various degrees of DM
11 thickening and dystrophic appearing cornea endothelial cells, with areas devoid of cells.
12

13 Immunofluorescence staining with the 5D4 antibody revealed increased staining of 5D4+ KS
14 throughout the full thickness of DM in the three probands, displaying a lamellated appearance
15 compared to controls. This lamellated appearance suggested that 5D4+ KS was continuously
16 deposited by the corneal endothelial cells over time. Lectin-FITC staining was also increased
17 in the DM samples from the three probands compared to the controls, with a laminated
18 appearance throughout the thickness of DM, particularly in the posterior zone/layers closer to
19 the corneal endothelium. A tumor tissue sample with neovascularization included as a
20 positive control for Lectin-FITC demonstrated staining of blood vessel basement membranes.
21 Alcian Blue staining demonstrated positive staining primarily in the posterior zone/layers of
22 the DM and in the cytoplasm of the remaining corneal endothelial cells in the three DM
23 samples. In contrast, control samples showed no Alcian Blue staining of the DM or corneal
24 endothelium. A sample of human colon adenocarcinoma included as a positive control
25 showed Alcian blue positive mucus droplets within colon epithelial cells. HID staining was
26 observed in corneal endothelial cells and/or in protruding nodules on the posterior surface of
27

428 DM in the three DM samples, whereas no HID staining was observed in controls, suggesting
429 that the gray deposits on the posterior aspect of the peripheral cornea observed clinically
7 may consist of low sulfated KS. A sample of healthy murine colon epithelium included as
10 positive control for HID staining demonstrated dark brown HID-stained mucus droplets within
12 the colon epithelial cells.
14

15 To evaluate the impact of the *CHST6* c.-690G>C mutation on systemic KS sulfation and
17 metabolism, serum and/or DBS were collected from affected and unaffected members of 6 of
18 19 families (Fig. 1). Control samples included serum samples from four healthy individuals, the
20 21 unrelated spouse of the proband in Family E, and two individuals with fleck corneal
22 23 dystrophy. The levels of di-sulfated KS, mono-sulfated KS, total sulfated KS (di-sulfated KS +
24 25 mono-sulfated KS), dermatan sulfate (DS), and heparan sulfate (HS) from serum samples
26 27 and DBS samples for each individual are presented in Tables 3 and 4, respectively. Adjusted
28 29 DBS measurements were provided for ease of comparison with serum sample
30 31 measurements, based on a previously published method.¹³ The blood sulfated KS levels in
32 33 most of the individuals examined, affected or unaffected, were within the range of sulfated KS
34 35 levels found in health controls.
36 37

38 39 4044 The above data suggested that the aberrant overexpression of 5D4+ high sulfated KS
41 42 induced by the *CHST6* c.-690G>C mutation was restricted to the corneal endothelium and
43 44 DM in the corneas of affected individuals. Additionally, low-sulfated KS and non-sulfated KS
45 46 were overexpressed in corneal endothelium and DM as well.
47 48 5051

52 53 5448 *CHST6* c.-690G>C is a pathogenic variant

55 56 575449 To determine the pathogenicity of the identified variants, we followed established guidelines
58 59 published by American College of Medical Genetics and Genomics (ACMG), Association for
60 61 62 63 64 65

2
3 Molecular Pathology (AMP) and UK Association for Clinical Genomic Science (ACGS). These
4 guidelines include the 2015 ACMG-AMP variant interpretation guidelines for Mendelian
5 disorders¹⁸, the 2018 ACMG/AMP guideline update for PP5 and BP6 variants¹⁹, the Bayesian
6 adaptation of the ACMG/AMP variant interpretation framework¹⁴, the 2020 ACMG/AMP
7 guideline update for PS3/BS3 criterion²⁰, and the 2022 ACGS variant interpretation guidelines
8 for non-coding variants.²¹ Four of the six identified variants, c.-690G>C, p.Arg211Gln,
9 p.Tyr268Cys, and p.Pro280Leu, can be classified as “Pathogenic”, each with a posterior
10 probability of 0.999 and a calculated OddsPath value of 13617, indicating that the pathogenic
11 evidence is “Very Strong” for all of these four variants (Table 5).

12

13

14

15

16

17

18

19

20

21

22

23

24

25

26

27

28

29

30

31

32

33

34

35

36

37

38

39

40

41

42

43

44

45

46

47

48

49

50

51

52

53

54

55

56

57

58

59

60

61

62

63

64

65

3
4 461 **DISCUSSION**
5

6 462 This study details the clinical, histopathologic, immunohistochemical and genetic features of a
7
8 463 *CHST6*-associated corneal endothelial dystrophy affecting seven unrelated families from
9
10 464 Vietnam and Thailand. The clinical presentation of this corneal endothelial dystrophy is
11
12 465 distinct from previously described corneal endothelial dystrophies, namely Fuchs endothelial
13
14 466 corneal dystrophy, congenital hereditary endothelial dystrophy, posterior polymorphous
15
16 467 corneal dystrophy and x-linked endothelial corneal dystrophy. We suggest the name
17
18 468 Peripheral macular endothelial dystrophy (PMED) to describe this dystrophy, given the similar
19
20 469 appearance of the peripheral gray-white deposits observed in PMED to those observed in
21
22 470 MCD. However, this dystrophy is sufficiently distinct from MCD in terms of clinical features,
23
24 471 surgical management, genetic basis, and the functional impact of associated mutations to be
25
26 472 considered as unique corneal dystrophy.
27
28

29 473 In terms of the clinical features, individuals with PMED initially present with discrete gray-
30
31 474 white deposits on the posterior aspect of the peripheral cornea, without stromal haze, stromal
32
33 475 opacities or associated visual symptoms. The peripheral deposits slowly increase in size and
34
35 476 number, extending in some individuals into the mid-peripheral cornea. Subsequently,
36
37 477 epithelial and/or stromal corneal edema can develop, which can be successfully managed
38
39 478 with endothelial keratoplasty.
40
41

42 479 Similar to MCD, PMED is associated with promoter and coding region mutations in *CHST6*.
43
44 480 Identified coding region mutations, p.Tyr268Cys (Y268C) and p.Arg211Gln (R211Q), have
45
46 481 been previously reported to be associated with MCD, suggesting these two coding mutations
47
48 482 lead to decreased CGn6ST/*CHST6* enzymatic activity.^{22 23} However, p.Pro280Leu (P280L)
49
50 483 is novel and has not been associated with MCD. In each of the seven families that we
51
52 484 describe, the rare *CHST6* promoter mutation c.-690G>C, not previously associated with
53
54
55
56
57
58
59
60
61
62
63
64
65

2
3 MCD, was identified in either the homozygous or compound heterozygous state. *In silico*
4 analysis suggests that *CHST6* c.-690G>C is located at the binding site of RNA polymerase II
5 in the *CHST6* promoter. In vitro functional analysis, together with DM histological findings and
6 serum KS measurement, suggest that the c.-690G>C mutation, either in the homozygous
7 state or in the compound heterozygous state with another *CHST6* coding mutation, leads to
8 increased CGn6ST-mediated sulfation of KS only in the corneal endothelium and minimally
9 affects the CGn6ST enzyme activity in keratocytes and other somatic cell types. Additionally,
10 our data suggests that *CHST6* c.-690G>C in the heterozygous state may be sufficient to
11 cause disease, given the observation of a few peripheral deposits without corneal edema in a
12 heterozygous individual and the in vitro functional analysis of c.-690G>C in heterozygous
13 state demonstrating increased CGn6ST-mediated KS sulfation in corneal endothelial cells.
14
15 The distinct functional effects of *CHST6* c.-690G>C in corneal endothelial cells versus in
16 keratocytes and other somatic cell types may be related to the variability of enhancer and
17 promoter usage across tissues and the highly tissue-specific effects of non-coding variants.
18 Because of such tissue-specific effects, the 2022 ACGS variant interpretation guidelines for
19 non-coding variants²¹ specified that functional assay(s) of identified non-coding variant(s)
20 need to be performed in disease-relevant tissues or cell types. In our study, functional assays
21 of identified *CHST6* non-coding (c.-690G>C) and coding (P280L and Y268C) mutations were
22 performed in HCEnC and HK using the same outcome measurement – the level of 5D4
23 antibody labeled highly sulfated KS. While the functional assay showed decreased 5D4+ KS
24 with the two *CHST6* coding mutations in HK and no apparent change of already low 5D4+ KS
25 in HCEnC, the assay also showed *CHST6* c.-690G>C enhanced 5D4+ KS in HCEnC with no
26 apparent effect in HK. These results provided strong evidence of the differential functional
27 consequences of *CHST6* c.-690G>C in keratocytes compared to corneal endothelium.

2 To the best of our knowledge, there have been three publications describing two individual
3 cases and a family with peripheral gray-white macular deposits at the level of DM. Chaurasia
4 et al. described a 67-year-old Indian woman who presented with corneal edema, guttae and
5 bilateral deposits at DM, scattered circumferentially in the peripheral cornea.²⁴ After a clinical
6 diagnosis of macular corneal dystrophy was made, without genetic confirmation, Descemet
7 stripping endothelial keratoplasty (DSEK) was performed in the left eye, with improvement of
8 20/50 preoperative visual acuity to 20/30. Histological examination in the excised DM
9 demonstrated Alcian blue-positive endothelial cells, consistent with the findings in the DM
10 from the three probands that we report. We previously described a 68-year-old Chinese man
11 with bilateral clear corneas, except for peripheral round gray-white discrete deposits at the
12 level of DM. Both eyes exhibited decreased central corneal thickness and normal endothelial
13 cell densities. CHST6 screening in this individual demonstrated two compound heterozygous
14 mutations *in trans* configuration: c.-26C>A, a non-coding mutation in exon 2 that created a
15 new upstream open reading frame (uORF'), predicted to attenuate translation efficiency of
16 the downstream main ORF; and c.803A>G, p.(Tyr268Cys), which is the same mutation
17 identified in Family C that we report. Serum KS levels were reduced compared to age-
18 matched controls, leading us to conclude that the diagnosis in this case was macular corneal
19 dystrophy type II.²⁵ However, when we performed an in vitro cell-based assay of the
20 compound heterozygous mutations identified in this individual, we observed increased
21 sulfated KS compared to wild type in HCEnC but no effect in HK (Supplemental Fig. 2),
22 similar to that observed with CHST6 c.-690G>C. Given this, and the absence of macular
23 stromal deposits and diffuse stromal haze that are essential phenotypic features of MCD, we
24 now believe that this individual more likely has PMED. Ye et al. described a Chinese
25 pedigree consisting of 13 members across 3 generations, including 6 affected individuals,
26

2 showing an autosomal dominant inheritance pattern.²⁶ The average age of disease onset was
3 16.5 years of age, and affected members demonstrated progressive enlargement and
4 coalescence of white translucent spots initially confined to the peripheral DM with subsequent
5 involvement of the central DM, with the development of endothelial decompensation,
6 manifest by corneal epithelial and stromal edema, in some individuals. While the reported
7 clinical features of this pedigree are similar to those of PMED, the authors identified a
8 heterozygous *KIAA1522* (c.1331G>A) variant that segregated with affected status in the
9 pedigree, indicating a distinct genetic basis from the families that we report.²⁶

10 With the elucidation of the genetic basis of essentially all of the corneal dystrophies and the
11 initiation of preclinical trials of gene therapy for selected corneal dystrophies, we propose to
12 reconsider the classification system of the corneal dystrophies, with more emphasis placed
13 on the genetic basis and less on the layer of the cornea that is primarily affected. The first
14 FDA-approved gene therapy, Luxturna®, received approval with a genetic indication labeling
15 "for the treatment of patients with confirmed biallelic *RPE65* mutation-associated retinal
16 dystrophy".²⁷ This wording was selected primarily based on the observed variety of clinical
17 diagnoses for *RPE65*-mediated inherited retinal diseases, despite common characteristic
18 findings such as nyctalopia. Depending on the time of disease onset, severity, rate of
19 progression and presenting phenotype, the most common diagnoses for *RPE65*-mediated
20 inherited retinal diseases include Leber congenital amaurosis (LCA), early-onset severe
21 retinal dystrophy (EOSRD), retinitis pigmentosa (RP), Fundus albipunctatus (FA) and
22 others.^{28,29} However, regardless of the clinical diagnosis, confirmation of biallelic *RPE65*
23 mutations is required for a patient to be eligible for Luxturna® gene therapy. Similarly, as the
24 *TGFB1* epithelial-stromal dystrophies demonstrate significant phenotypic heterogeneity and
25 involve multiple layers of the cornea, they are more accurately classified and conceptualized

2
3 using a molecular genetic rather than an anatomic construct. Given the fact that both MCD
4 and PMED are associated with promoter and coding region mutations in *CHST6*, we propose
5
6 that they should both be categorized as *CHST6*-associated corneal dystrophies. The shifting
7 of the emphasis from variable phenotypic features to the invariant underlying genetic defects
8 associated with the corneal dystrophies is a natural and necessary evolution as we enter the
9 era of genetic therapy for corneal dystrophies.
10
11
12
13
14
15
16
17
18
19
20
21
22
23
24
25
26
27
28
29
30
31
32
33
34
35
36
37
38
39
40
41
42
43
44
45
46
47
48
49
50
51
52
53
54
55
56
57
58
59
60
61
62
63
64
65

4 **AUTHOR CONTRIBUTIONS**564 **Wenlin Zhang:** Conceptualization, Methodology, Formal Analysis, Investigation, Data

565 Curation, Writing-Original Draft, Writing-Review & editing, Visualization, Project

566 Administration. **Huong Duong:** Conceptualization, Validation, Investigation, Data Curation,567 Writing-Review & editing, Supervision, Project Administration. **Passara Jongkhajornpong:**568 Conceptualization, Validation, Investigation, Data Curation, Writing-Review & editing. **Do Thi**569 **Thuy Hang:** Validation, Investigation, Data Curation. **Huan Pham:** Validation, Investigation,570 Data Curation. **Mai Nguyen:** Validation, Investigation, Data Curation. **Charlene Choo:**571 Validation, Investigation, Data Curation. **Dominic Williams:** Investigation, Data Curation572 **Xuan Nguyen:** Investigation, Data Curation. **Tien Dat Nguyen:** Investigation, Data Curation.573 **Brian Aguirre:** Investigation, Data Curation. **Shaukat Khan:** Investigation, Data Curation.574 **Madhuri Wadehra:** Supervision, **Shunji Tomatsu:** Methodology, Writing-Review & editing,575 Supervision, Project Administration. **Anthony J. Aldave:** Conceptualization, Methodology,

576 Writing-Review & editing, Supervision, Project Administration. Funding Acquisition.

4 **ACKNOWLEDGEMENTS/DISCLOSURE**

5
6 Funding: This work was supported by the National Eye Institute P30EY000331 (core grant to
7
8 the Stein Eye Institute), and an unrestricted grant from Research to Prevent Blindness (Stein
9
10 Eye Institute)

11
12 Financial Disclosures: No financial disclosures

13
14 We thank Dr. Tomoya O. Akama (Kansai Medical University) for the generous gifts of
15
16 pcDNA3_CGn6ST, pcDNA3_KSG6ST and pcDNA3_b3GnT7 plasmids, Dr. James V. Jester
17
18 (UC Irvine) for the generous gift of a telomerase immortalized human keratocyte cell line and
19
20 Dr. Ula V. Jurkunas (Massachusetts Eye and Ear) for the generous gift of a telomerase
21
22 immortalized human endothelial cell line.

23

24

25

26

27

28

29

30

31

32

33

34

35

36

37

38

39

40

41

42

43

44

45

46

47

48

49

50

51

52

53

54

55

56

57

58

59

60

61

62

63

64

65

4 REFERENCES

- 5
6
7
8
9
10 Weiss JS, Moller HU, Aldave AJ, et al. IC3D classification of corneal dystrophies--edition 2.
11 Cornea. 2015;34(2):117-159.
- 12 Weiss JS, Rapuano CJ, Seitz B, et al. IC3D Classification of Corneal Dystrophies-Edition 3.
13 Cornea. 2024;43(4):466-527.
- 14 Bendl J, Musil M, Stourac J, Zendulka J, Damborsky J, Brezovsky J. PredictSNP2: A Unified
15 Platform for Accurately Evaluating SNP Effects by Exploiting the Different Characteristics of Variants
16 in Distinct Genomic Regions. *PLoS Comput Biol.* 2016;12(5):e1004962.
- 17 Adzhubei IA, Schmidt S, Peshkin L, et al. A method and server for predicting damaging
18 missense mutations. *Nature methods.* 2010;7(4):248-249.
- 19 Boyle AP, Hong EL, Hariharan M, et al. Annotation of functional variation in personal genomes
20 using RegulomeDB. *Genome Res.* 2012;22(9):1790-1797.
- 21 Abascal F, Acosta R, Addleman NJ, et al. Expanded encyclopaedias of DNA elements in the
22 human and mouse genomes. *Nature.* 2020;583(7818):699-710.
- 23 Zhou J, Theesfeld CL, Yao K, Chen KM, Wong AK, Troyanskaya OG. Deep learning
24 sequence-based ab initio prediction of variant effects on expression and disease risk. *Nature*
25 Genetics. 2018;50(8):1171-1179.
- 26 Consortium EP, Moore JE, Purcaro MJ, et al. Expanded encyclopaedias of DNA elements in
27 the human and mouse genomes. *Nature.* 2020;583(7818):699-710.
- 28 Akama TO, Nakayama J, Nishida K, et al. Human corneal GlcNac 6-O-sulfotransferase and
29 mouse intestinal GlcNac 6-O-sulfotransferase both produce keratan sulfate. *J Biol Chem.*
30 2001;276(19):16271-16278.
- 31 Schmedt T, Chen Y, Nguyen TT, Li S, Bonanno JA, Jurkunas UV. Telomerase immortalization
32 of human corneal endothelial cells yields functional hexagonal monolayers. *PLoS One.*
33 2012;7(12):e51427.

- 2
3 11. Jester JV, Huang J, Fisher S, et al. Myofibroblast differentiation of normal human keratocytes
4 and hTERT, extended-life human corneal fibroblasts. *Invest Ophthalmol Vis Sci.* 2003;44(5):1850-
5 1858.
6
7 12. Tomatsu S, Shimada T, Mason RW, et al. Establishment of glycosaminoglycan assays for
8 mucopolysaccharidoses. *Metabolites.* 2014;4(3):655-679.
9
10 13. Kubaski F, Suzuki Y, Orii K, et al. Glycosaminoglycan levels in dried blood spots of patients
11 with mucopolysaccharidoses and mucolipidoses. *Mol Genet Metab.* 2017;120(3):247-254.
12
13 14. Tavtigian SV, Greenblatt MS, Harrison SM, et al. Modeling the ACMG/AMP variant
14 classification guidelines as a Bayesian classification framework. *Genet Med.* 2018;20(9):1054-1060.
15
16 15. Brnich SE, Rivera-Munoz EA, Berg JS. Quantifying the potential of functional evidence to
17 reclassify variants of uncertain significance in the categorical and Bayesian interpretation frameworks.
18
19 16. Harrison SM, Biesecker LG, Rehm HL. Overview of Specifications to the ACMG/AMP Variant
20 Interpretation Guidelines. *Curr Protoc Hum Genet.* 2019;103(1):e93.
21
22 17. Akama TO, Nishida K, Nakayama J, et al. Macular corneal dystrophy type I and type II are
23 caused by distinct mutations in a new sulphotransferase gene. *Nat Genet.* 2000;26(2):237-241.
24
25 18. Richards S, Aziz N, Bale S, et al. Standards and guidelines for the interpretation of sequence
26 variants: a joint consensus recommendation of the American College of Medical Genetics and
27 Genomics and the Association for Molecular Pathology. *Genet Med.* 2015;17(5):405-424.
28
29 19. Biesecker LG, Harrison SM. The ACMG/AMP reputable source criteria for the interpretation of
30 sequence variants. *Genetics in Medicine.* 2018;20(12):1687-1688.
31
32 20. Brnich SE, Abou Tayoun AN, Couch FJ, et al. Recommendations for application of the
33 functional evidence PS3/BS3 criterion using the ACMG/AMP sequence variant interpretation
34 framework. *Genome Medicine.* 2019;12(1):3.
35
36 21. Ellingford JM, Ahn JW, Bagnall RD, et al. Recommendations for clinical interpretation of
37 variants found in non-coding regions of the genome. *Genome Medicine.* 2022;14(1):73.

- 2
3 638 22. Liu Z, Tian X, Iida N, et al. Mutation analysis of CHST6 gene in Chinese patients with macular
4 corneal dystrophy. *Cornea*. 2010;29(8):883-888.
5
6 639 23. Gruenauer-Kloevekorn C, Braeutigam S, Heinritz W, Froster UG, Duncker GI. Macular corneal
7 dystrophy: mutational spectrum in German patients, novel mutations and therapeutic options. *Graefes
8 Arch Clin Exp Ophthalmol*. 2008;246(10):1441-1447.
9
10 640 24. Chaurasia S, Mishra DK. Atypical presentation of macular corneal dystrophy managed by
11 Descemet stripping endothelial keratoplasty. *Indian J Ophthalmol*. 2019;67(1):118-119.
12
13 641 25. Zhang W, Kassels AC, Barrington A, et al. Macular corneal dystrophy with isolated peripheral
14 Descemet membrane deposits. *Am J Ophthalmol Case Rep*. 2019;16:100571.
15
16 642 26. Ye M, Lu Q, Zhao D, et al. New Endothelial Corneal Dystrophy in a Chinese Family. *Cornea*.
17 2023;42(5):529-535.
18
19 643 27. LUXURNA (voretigene neparvovec-rzyl) intraocular suspension for subretinal injection
20 [package insert]. Philadelphia, PA: Spark Therapeutics, Inc.; 2022.
21
22 644 28. Maguire AM, Bennett J, Aleman EM, Leroy BP, Aleman TS. Clinical Perspective: Treating
23 RPE65-Associated Retinal Dystrophy. *Mol Ther*. 2021;29(2):442-463.
24
25 645 29. Sodi A, Banfi S, Testa F, et al. RPE65-associated inherited retinal diseases: consensus
26 recommendations for eligibility to gene therapy. *Orphanet Journal of Rare Diseases*. 2021;16(1):257.
27
28 646
29
30 647
31
32 648
33
34 649
35
36 650
37
38 651
39
40 652
41
42 653
43
44 654
45
46
47
48
49
50
51
52
53
54
55
56
57
58
59
60
61
62
63
64
65

4 **FIGURE CAPTIONS**

5
6 **Figure 1. Pedigrees of seven previously unreported families with Peripheral macular**
7 **endothelial dystrophy (PMED).** Family A is Thai, families B – G are Vietnamese. The
8 arrowhead indicates the proband in each family. Asterisks indicate enrolled individuals that
9 were examined and had genomic DNA collected. Filled symbols indicate affected individuals,
10 empty symbols indicate unaffected individuals. Question marks (?) indicate individuals who
11 were not examined and are of undetermined affected status. Diagonal lines mark deceased
12 individuals. “WES” indicates individuals in whom whole exome sequencing was performed.
13 Red dot “•” indicates individuals from whom dried blood spots were collected for measurement
14 of sulfated GAGs. Red “drop shape” indicates individuals from whom serum was collected for
15 measurement of sulfated GAGs. “EK” indicates individuals in whom endothelial keratoplasty
16 was performed in at least one eye.

17
18 **Figure 2. Clinical findings of affected individuals in Families A (panels A-C), B (D-G) and**
19 **C (H-J).** (A) Slit lamp photomicrographs of the proband. (B) Slit lamp photomicrographs of the
20 proband following DMEK in both eyes. (C) Slit lamp photomicrographs of the affected mother
21 of the proband. (D) Slit lamp photomicrographs of the proband at initial presentation and (E)
22 six months following presentation. (F) Slit lamp photos of the proband following DSAEK in the
23 right eye. (G) Slit lamp photomicrographs of the proband’s older brother. (H) Slit lamp
24 photomicrographs of the proband at presentation. (I) Slit lamp photomicrographs of the
25 proband’s left eye following DMEK. (J) Slit lamp photos of the proband’s affected older sister.

26
27 **Figure 3. Clinical findings of affected individuals in Families D (panels A-D), E (E-F), F**
28 **(G-H) and G (I).** (A) Slit lamp photomicrographs of the proband at presentation. (B) AS-OCT
29 images of the proband at presentation. (C) Slit lamp photomicrographs of one of the proband’s

2 affected younger brothers. (D) Slit lamp photomicrographs of the other affected younger
3 brother of the proband. (E) Slit lamp photomicrographs of the proband at presentation. (F) Slit
4 lamp photomicrographs of the affected younger sister of the proband. (G) Slit lamp
5 photomicrographs of the proband at presentation. (H) Slit lamp photomicrographs of the
6 proband's left eye following DSEK. (I) Slit lamp photomicrographs of the proband.
7
8
9
10
11
12
13
14
15
16
17
18
19
20
21
22
23
24
25
26
27
28
29
30
31
32
33
34
35
36
37
38
39
40
41
42
43
44
45
46
47
48
49
50
51
52
53
54
55
56
57
58
59
60
61
62
63
64
65

Figure 4. Functional Assay of CHST6 Mutants. (A) Graphical representation of *CHST6* gene structure and map of *CHST6* promoter-containing expressing vector pcDNA3_CGn6STwPro, showing the relative positions of *CHST6* exon 1 – 3 on the genome and in the vector. Color-coded lines depicted the relative positions of generated mutations in the vector. (B) Western Blot results of HCEnC and HK cell lysates following CGn6STwPro transfections. The amount of wild-type (WT) or mutant CGn6STwPro expression vector used was denoted as “2 \times ” for 250 ng / well and “1 \times ” for 125 ng / well. (C) Bar graph summary of 5D4+ KS relative fold change in HCEnC or HK transfected with mutant CGn6STwPro expression vectors when compared to WT/WT transfection.

Figure 5. Histology and immunohistochemistry of DM from three probands. Healthy control cornea: full thickness eye bank donor cornea. PCE DM: DM from an individual with pseudophakic corneal edema.

Table 1. Identified presumed pathogenic CHST6 mutations in families A – G

Family	Generation	Age	Affected Status	Allele 1	Allele 2
A	I-1	74	No	c.839C>T, p.(Pro280Leu) ¹	-
	I-2	73	Yes	-	n.-97G>C, c.-690G>C ^{2,5}
	II-1	52	No	-	n.-97G>C, c.-690G>C
	► II-2	50	Yes	c.839C>T, p.(Pro280Leu)	n.-97G>C, c.-690G>C
	III-1	25	No	-	n.-97G>C, c.-690G>C
B	► II-1	49	Yes	n.-97G>C, c.-690G>C	n.-97G>C, c.-690G>C
	II-2	45	Yes	n.-97G>C, c.-690G>C	n.-97G>C, c.-690G>C
	III-1	23	No	n.-97G>C, c.-690G>C	-
C	II-1	72	Yes	c.803A>G, p.(Tyr268Cys) ³	n.-97G>C, c.-690G>C
	II-4	66	No	-	n.-97G>C, c.-690G>C
	► II-5	60	Yes	c.803A>G, p.(Tyr268Cys)	n.-97G>C, c.-690G>C
	II-6	56	No	-	n.-97G>C, c.-690G>C
	II-7	52	No	-	n.-97G>C, c.-690G>C
	III-1	40	No	c.803A>G, p.(Tyr268Cys)	-
	III-2	37	No	-	n.-97G>C, c.-690G>C
	III-3	35	No	-	-
	III-4	33	No	c.803A>G, p.(Tyr268Cys)	-
	III-5	30	No	-	n.-97G>C, c.-690G>C
D	I-1	64	No	c.632G>A, p.(Arg211Gln) ⁴	-
	► II-1	41	Yes	c.632G>A, p.(Arg211Gln)	n.-97G>C, c.-690G>C
	II-2	39	No	-	-
	II-3	36	Yes	c.632G>A, p.(Arg211Gln)	n.-97G>C, c.-690G>C
	II-4	34	No	-	-
	II-5	31	Yes	c.632G>A, p.(Arg211Gln)	n.-97G>C, c.-690G>C
	II-6	28	No	-	n.-97G>C, c.-690G>C
	II-7	24	No	-	-
	III-1	8	No	c.632G>A, p.(Arg211Gln)	-
	III-3	20	No	-	-
E	► II-1	54	Yes	n.-97G>C, c.-690G>C	n.-97G>C, c.-690G>C
	II-2	42	Yes	n.-97G>C, c.-690G>C	n.-97G>C, c.-690G>C
F	► I-1	62	Yes	c.632G>A, p.(Arg211Gln)	n.-97G>C, c.-690G>C
	II-1	29	No	c.632G>A, p.(Arg211Gln)	-
G	► I-1	58	Yes	n.-97G>C, c.-690G>C	n.-97G>C, c.-690G>C
	II-1	25	No	n.-97G>C, c.-690G>C	-

► indicates proband. ¹rs201767298, no MAF; ²rs1009794816, MAF: 0.000064 (GnomAD), 0.000088 (TOPMED); ³rs72547539, MAF: 0.000064 (GnomAD), 0.000009 (ExAC), 0.00004 (TOPMED), 0.0002 (1000Genome), previously reported to be associated with MCD ¹⁶; ⁴rs771397083, MAF: 0.000004 (GnomAD), 0 (ExAC), previously reported to be associated with MCD ¹⁷; ⁵All screened individuals with a c.-690G>C mutation also carry two adjacent common variants *in cis*: c.-668C>T (rs2550323, TOPMED MAF 0.034) and c.-792C>T (rs2550322, TOPMED MAF 0.114)

Table 2. *In silico* analysis of identified *CHST6* mutations

Mutation	dbSNP IDS	RegulomeDB ¹			PredictSNP2 ²		PolyPhen-2 ³	
		Rank	Score	ChIP Data ⁴	Prediction	Score	Prediction	Score
c.-792C>T	rs2550322	4 ⁵	0.6091	EZH2 ⁷ (3/17)	-	-	-	-
c.-690G>C	rs1009794816	2b ⁶	1.0000	POLR2A ⁸ (10/36)	-	-	-	-
c.-668C>T	rs2550323	2b	0.5574	POLR2A (11/37)	-	-	-	-
p.Arg211Gln	rs771397083	-	-		Deleterious	1	Probably Damaging	1.0
p.Tyr268Cys	rs72547539	-	-		Deleterious	1	Probably Damaging	1.0
p.Pro280Leu	rs201767298	-	-		Deleterious	1	Probably Damaging	1.0

¹RegulomeDB version 2.0.3 was used. RegulomeDB probability score ranges from 0 to 1, with 1 being most likely to be a regulatory variant;

²PredictSNP2 score ranges from 0 to 1, with 1 being the most likely to be deleterious variant; ³PolyPhen-2 score ranges from 0.0 to 1.0. Variants with scores of 0.0 are predicted to be benign. Values closer to 1.0 are more confidently predicted to be deleterious; ⁴Column “ChIP Data” listed the most frequently bond transcriptional factor (TF) and/or subunit of transcriptional machinery for the variant coordinate Numbers in parenthesis are # of CHIP-seq data sets showing peak of listed TF or subunit / total # of CHIP-seq data sets with peak at the variant coordinate; ⁵RegulomeDB rank 4 represents “TF binding + DNase peak” as supporting data for the variant coordinate; ⁶RegulomeDB rank 2b represents “TF binding + any motif + DNase Footprint + DNase peak” as supporting data for the variant coordinate; ⁷EZH2, enhancer of zeste homolog 2, is a histone-lysine N-methyltransferase enzyme; ⁸POLR2A, RNA polymerase II subunit A, is the largest subunit of RNA polymerase II - the polymerase responsible for synthesizing messenger RNA in eukaryotes

Table 3. Serum glycosaminoglycan levels in enrolled individuals with and without PMED

Family ID Individual ID	Age ¹ (yrs)	Affected Status	KS (ng/ml)			DS (ng/ml)	HS (ng/ml)		
			Di-S KS ²	Mono-S KS ³	Total sulfated KS		ΔDiHS-NS ⁵	ΔDiHS-oS ⁶	
Healthy Control	1	62	150.9	301.4	452.3	17.9	6.0	36.8	
	2	57	122.0	325.3	447.4	13.1	7.0	56.8	
	3	59	158.7	317.2	475.9	15.0	8.2	57.9	
	4	60	120.4	282.2	402.5	21.2	12.9	74.3	
	5 ⁷	56	83.8	278.6	362.4	1.5	0.6	5.0	
	6 ⁸	57	78.3	160.8	239.1	28.5	11.5	93.5	
	7 ⁸	44	70.6	239.1	210.9	21.8	12.6	97.9	
	Mean (± 2 SD) (± 1.5 SD)	56	112.1 (41.3 – 182.9)	258.0 (106.9 – 409.0)	370.1 (157.9 – 582.3)	17.0 (4.3 – 29.8)	8.4 (1.8 – 15.0)	60.3 (11.5 – 109.1)	
B	► II-1	52	Yes	133.0	312.7	445.8	6.4	11.9	90.5
	I-1	64	No	88.6	142.3	230.9	12.8	14.1	113.6 ↑
	► II-1	41	Yes	59.5	194.1	253.6	0.2 ↓	1.4 ↓	5.6 ↓
D	II-2	39	No	70.3	141.4	211.7	7.3	9.5	83.2
	II-3	36	Yes	97.9	171.0	268.9	5.1	11.2	100.2
	II-4	34	No	87.7	163.4	251.1	5.4	19.2 ↑	88.0
	II-5	31	Yes	47.3	112.4	159.7	8.9	14.2	102.8
	II-6	28	No	89.6	218.2	307.8	4.1 ↓	8.6	68.8
	II-7	24	No	104.4	226.8	331.2	5.1	11.2	92.0
	III-3	20	No	106.0	285.3	391.3	9.2	9.0	89.0
	III-4	12	No	143.7	469.9	613.6	7.2	12.6	108.1
E	► II-1	54	Yes	35.2 ↓	114.7	149.9 ↓	0.9 ↓	0.5	5.2
	II-2	42	Yes	55.1	177.8	232.9	0.2 ↓	0.6	5.0
F	► I-1	62	Yes	66.7	145.8	212.5	0.1 ↓	0.8	6.6
G	► I-1	58	Yes	107.8	170.7	278.6	2.3	8.4	65.8
	II-1	25	No	78.9	167.2	246.2	6.5	7.8	67.6

► indicates proband. Measurement values outside of “mean ± 2 SD (1.5 SD)” of healthy control values were annotated with downward arrow ↓ or upward arrow ↑. ¹Age at serum sample collection; ²Di-S KS: di-sulfated KS, Gal(6S)β1 → 4GlcNAc(6S); ³Mono-S KS: mono-sulfated KS, Galβ1 → 4GlcNAc(6S); ⁴ΔDi-4S [ΔHexUAα1-4GlcNAc(4-O-sulfate)]: 2-acetamido-2-deoxy-4-O-(4-deoxy-a-L-threohex-4-enopyranosyluronic acid)-4-O-sulfo-D-glucose; ⁵ΔDiHS-NS [ΔHexUAα1-4GlcN(2-N-sulfate)]: 2-deoxy-2-sulfamino-4-O-(4-deoxy-a-L-threo-hex-4-enopyranosyluronic acid)-D-glucose; ⁶ΔDiHS-oS (ΔHexUAα1-4GlcNAc): 2-acetamido-2-deoxy-4-O-(4-deoxy-a-L-threo-hex-4-nopyranosyluronic acid) -D-glucose; ⁷Spouse of individual II-2 from family E; ⁸Individuals clinically diagnosed with Fleck Corneal Dystrophy

Table 4. DBS glycosaminoglycan levels in enrolled individuals with and without PMED

Family ID Individual ID	Age ¹ (yrs)	Affected Status	KS (ng/ml)			DS (ng/ml)	HS (ng/ml)		
			Di-S KS ²	Mono-S KS ³	Total sulfated KS		ΔDi-4S ⁴	ΔDiHS-NS ⁵	ΔDiHS-oS ⁶
CTRL	Mean (± 2 SD) (± 1.5 SD)	56 N/A	112.1 (41.3 – 182.9)	258.0 (106.9 – 409.0)	370.1 (157.9 – 582.3)	17.0 (4.3 – 29.8)	8.4 (1.8 – 15.0)	60.3 (11.5 – 109.1)	
A	I-1	74	No	158.7	157.6	316.3	32.6 ↑	7.5	49.5
	I-2	73	Yes	75.6	154.9	230.5	53.9 ↑	8.5	65.9
	II-1	52	No	119.4	149.7	269.1	46.7 ↑	6.5	50.9
	► II-2	50	Yes	68.3	106.4 ↓	174.7	45.0 ↑	5.8	55.1
	III-1	25	No	81.1	148.7	229.8	45.6 ↑	7.2	64.0
D	► II-1	41	Yes	81.4	164.4	245.8	15.8	7.2	57.1
E	► II-1	54	Yes	91.1	156.0	247.1	1.5	7.7	66.4
	II-2	42	Yes	66.0	113.3	179.3	6.0	9.7	38.2
F	► I-1	62	Yes	107.8	131.9	239.7	17.2	5.6	68.8

► indicates proband. Measurement values outside of “mean ± 2 SD (1.5 SD)” of healthy control values were annotated with downward arrow ↓ or upward arrow ↑. ¹Age at DBS sample collection; ²Di-S KS: di-sulfated KS, Gal(6S)β1 → 4GlcNAc(6S); ³Mono-S KS: mono-sulfated KS, Galβ1 → 4GlcNAc(6S); ⁴ΔDi-4S [ΔHexUAα1–4GlcNAc(4-O-sulfate)]: 2-acetamido-2-deoxy-4-O-(4-deoxy-a-L-threohex-4-enopyranosyluronic acid)-4-O-sulfo-D-glucose; ⁵ΔDiHS-NS [ΔHexUAα1–4GlcN(2-N-sulfate)]: 2-deoxy-2-sulfamino-4-O-(4-deoxy-a-L-threo-hex-4-enopyranosyluronic acid)-D-glucose; ⁶ΔDiHS-oS (ΔHexUAα1–4GlcNAc): 2-acetamido-2-deoxy-4-O-(4-deoxy-a-L-threo-hex-4-nopyranosyluronic acid) -D-glucose

Table 5. ACMG/AMP guideline scoring of identified *CHST6* variants

Identified <i>CHST6</i> Variant	Pathogenic Criteria Satisfied	Benign Criteria Satisfied	Combined OddsPath ¹	<i>Post_P</i>	Classification Determination
c.-792C>T	PP1, PP3, PP4	BA1	0.001	0.000	Benign
c.-690G>C	PS3, PS4, PM3, PP1, PP3, PP4		13617.914	0.999	Pathogenic
c.-668C>T	PP1, PP4	BS1, BP4	0.053	0.006	Likely benign
c.632G>A, p.Arg211Gln	PS1, PS4, PM2, PP1, PP3, PP4		13617.914	0.999	Pathogenic
c.803A>G, p.Tyr268Cys	PS1, PS4, PM2, PP1, PP3, PP4		13617.914	0.999	Pathogenic
c.839C>T, p.Pro280Leu	PS3, PS4, PM2, PP1, PP3, PP4		13617.914	0.999	Pathogenic

¹OddsPath ratio cut-off values for Supporting, Moderate, Strong, and Very Strong pathogenic evidence are 2, 4.3, 18.7, and 350, respectively¹³

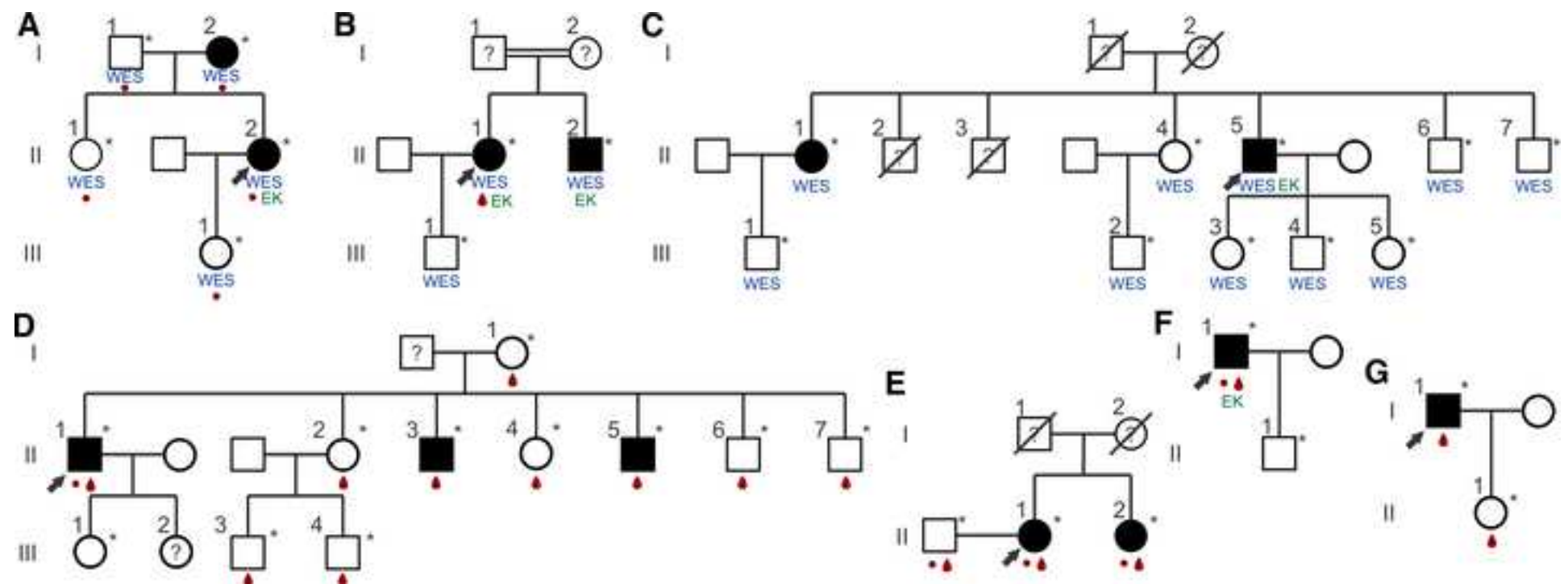


Figure 2

Click here to access/download; Figure - label number in Description field; no PDFs; Figure 2 v4.tif

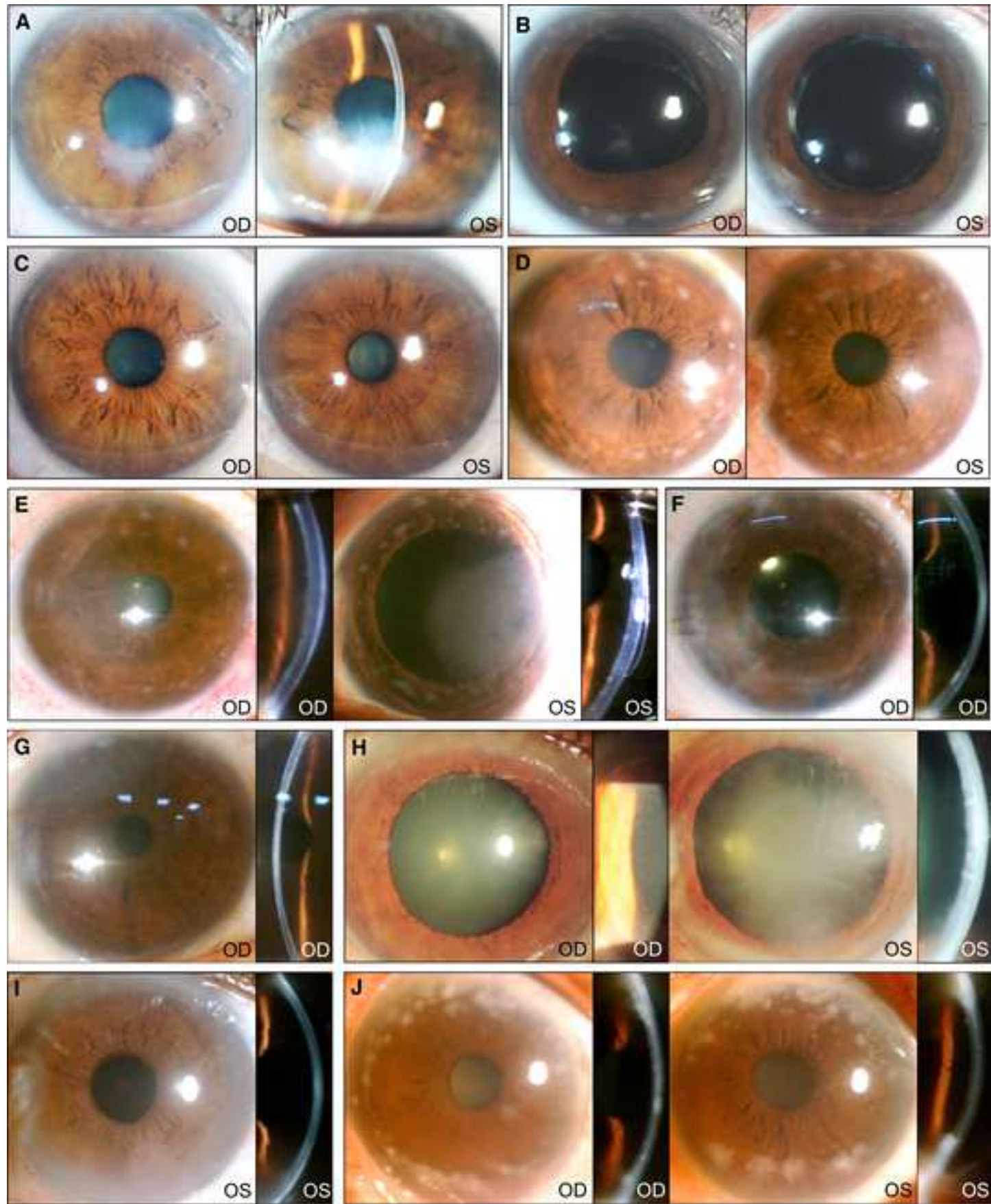


Figure 3

Click here to access/download; Figure - label number in Description field; no PDFs; Figure 3 v3.tif

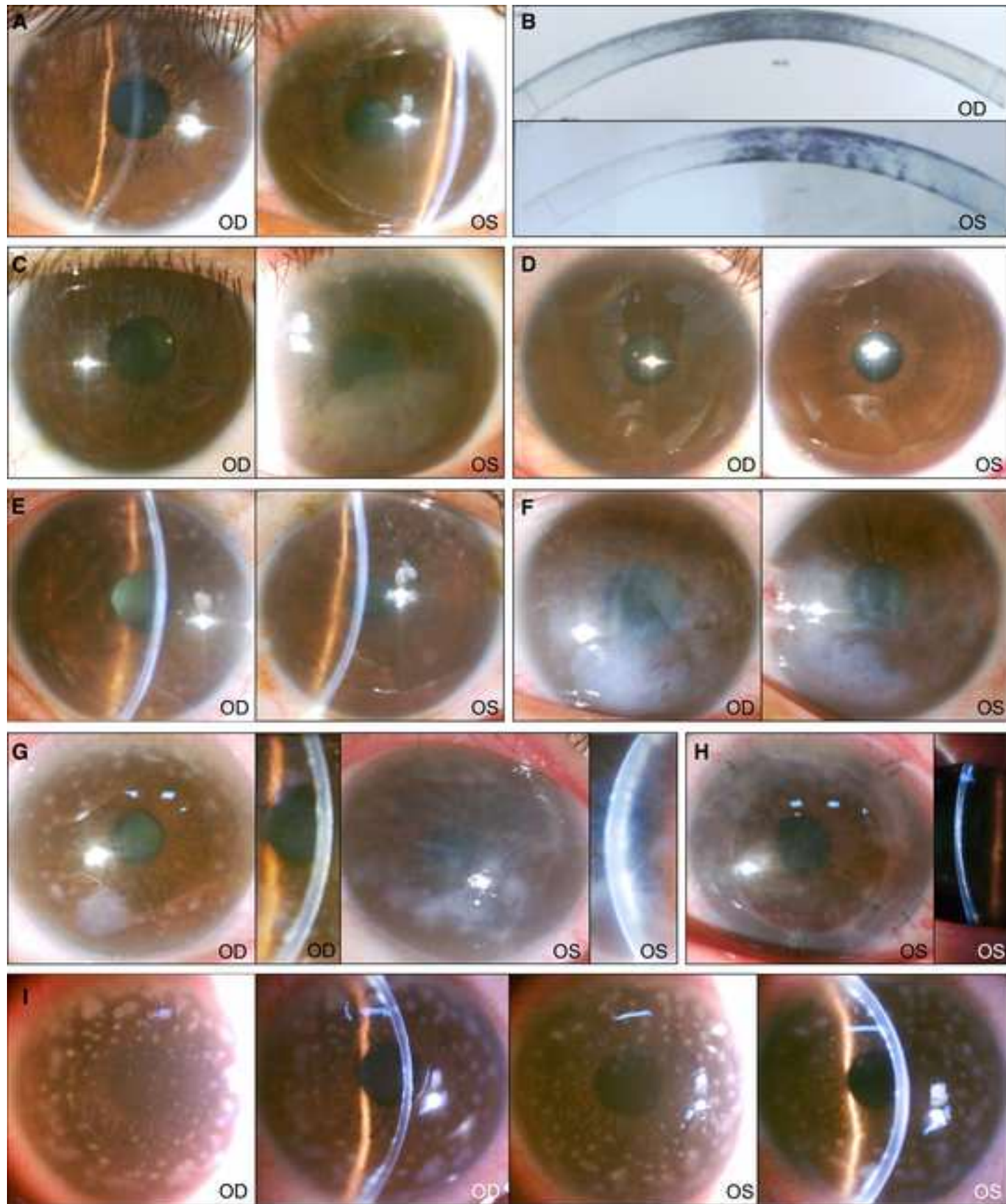


Figure 4

[Click here to access/download;Figure - label number in Description field; no PDFs;Figure 4 v2.tif](#)

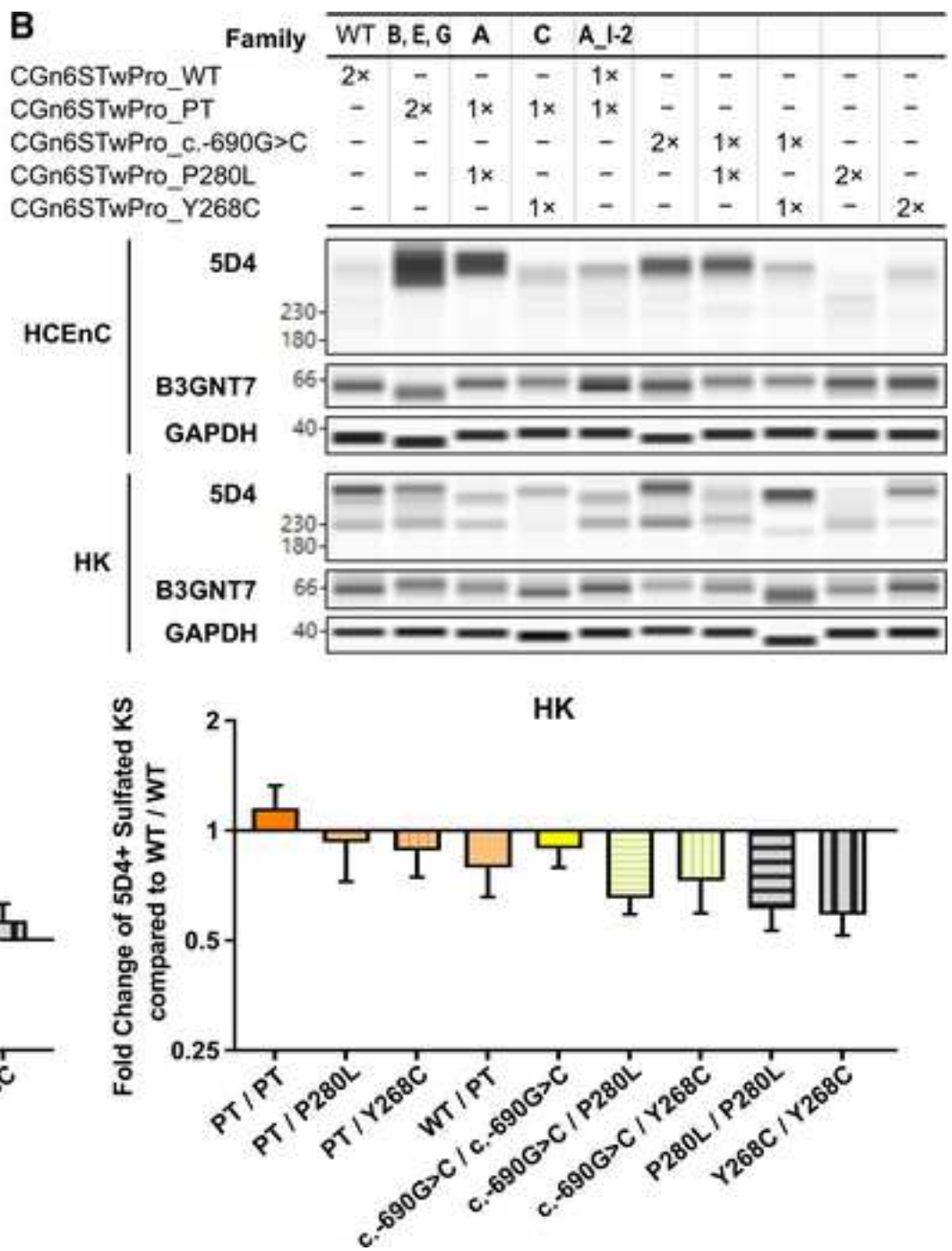
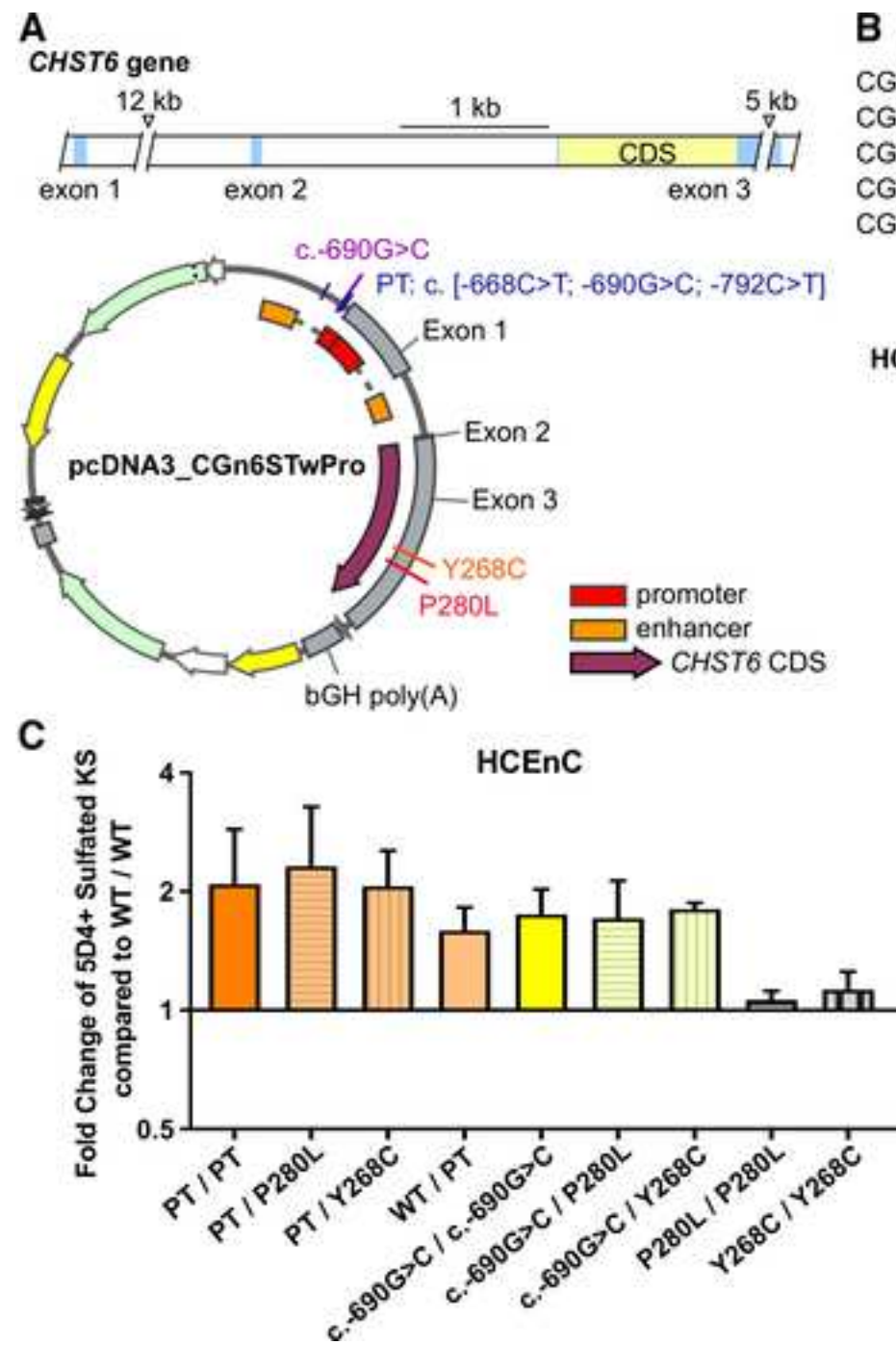
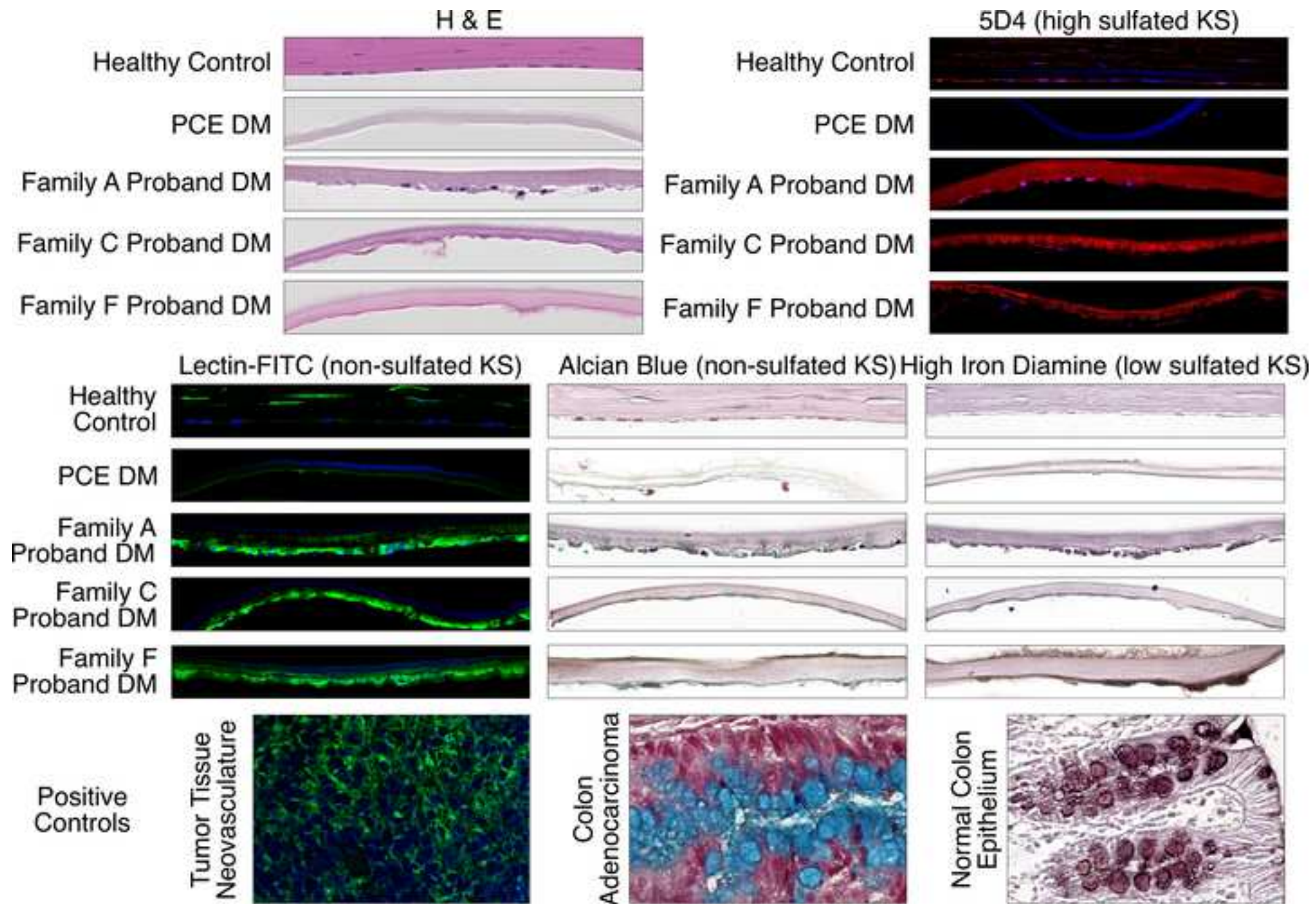


Figure 5

[Click here to access/download; Figure - label number in Description field; no PDFs; Figure 5 v3.tif](#)



Peripheral macular endothelial dystrophy is a novel *CHST6*-associated corneal dystrophy characterized by peripheral posterior corneal macular opacities and endothelial dysfunction without stromal haze or opacities.

1 **SUPPLEMENTAL MATERIALS**

2 *Primers and PCR conditions used for CHST6 screening*

3 PCR reactions were performed using GoTaq® Green Master Mix (Promega) with the
4 following conditions: initialization at 95°C for 3 minutes; 40 cycles of denaturing (95°C for
5 30 seconds), annealing (60 - 65°C for 30 seconds (see **Supplemental Table 1** for primer
6 set-specific annealing temperatures)), and extension (72° for 35 seconds); and final
7 elongation at 72°C for 5 minutes. Prior to sequencing, each amplicon was purified by
8 treatment with Exonuclease I and Shrimp Alkaline Phosphatase (USB Corp.), followed by
9 incubation at 37°C for 15 minutes and inactivation at 80°C for 15 minutes. Sanger
10 sequencing of the purified PCR template was then performed (Laragen Inc., Culver City,
11 CA). Replacement and deletion mutations upstream of *CHST6* were detected by PCR
12 followed by gel electrophoresis using primer combinations F1-R1, F1-R1M, F2-R2 and
13 F2M-R2, as described previously.^{16, 29}

14 *GATK variant calling*

15 Aligned sequences were marked with duplication and underwent base quality score
16 recalibration (BQSR). Variant calling of base quality score recalibrated sequences was
17 performed with GATK HaplotypeCaller in GVCF mode, followed by variant quality score
18 recalibration (VQSR). Genotype posterior was calculated and low-quality variants
19 (Genotype Quality (GQ) < 20) were labeled. Any possible *de novo* variant in family trios
20 was marked. Variants were labeled with dbSNP ID, and variants that were present only
21 in unaffected individuals and not present in any affected individuals were removed.
22 Common variants (MAF > 0.01) were removed based on global MAF in gnomAD,
23 1000Genome, TOPMED, ExAC and UK10K databases. Common variants in the South

24 Asian population were also removed, based on South Asian MAF in gnomeAD r3.0 and
25 1000Genome databases. All computations were performed on the UCLA Hoffman2
26 Cluster.

27 *WES variant filtration*

28 All enrolled individuals from Families A, B, and C underwent WES. However, Family C
29 was used as the index family as it contained the largest number of recruited individuals
30 among the three families that underwent WES. Variants were first filtered to retain only
31 novel or rare non-synonymous coding variants and splice region variants. Retained
32 candidate variants were then further filtered under the following two scenarios: assuming
33 autosomal recessive inheritance in Family C, homozygous or compound heterozygous
34 variants in the same gene that segregated with the affected status in Family C; and
35 assuming autosomal dominant inheritance in Family C, heterozygous variants that
36 segregated with the affected status in Family C. Genes containing homozygous or
37 compound heterozygous variants that segregated with the affected status in Family C
38 were then screened in affected and unaffected members of Families A and B to determine
39 segregation with the affected phenotype. Similarly, genes containing heterozygous
40 variants that segregated with the affected status in Family C were then screened in
41 affected and unaffected members of Families A and B to determine segregation with the
42 affected phenotype.

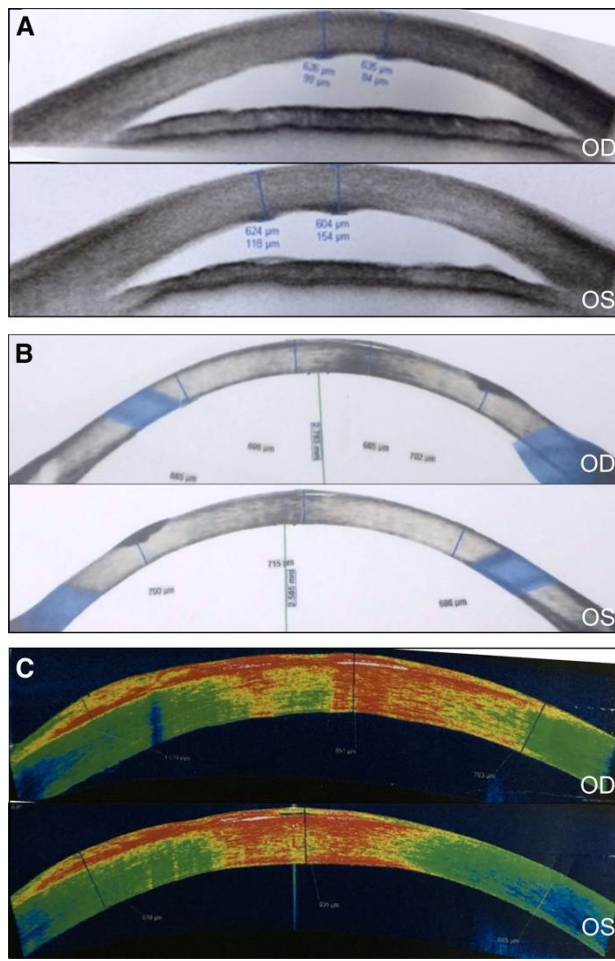
43 *Human corneal endothelial cell line cell culture*

44 A telomerase immortalized human corneal endothelial cell line (HCEnC) was cultured in
45 a 1:1 mixture of F12-Ham's medium and M199 medium, supplemented with 5% fetal
46 bovine serum (Corning), 20 µg/mL human recombinant insulin (Thermo Fisher Scientific),

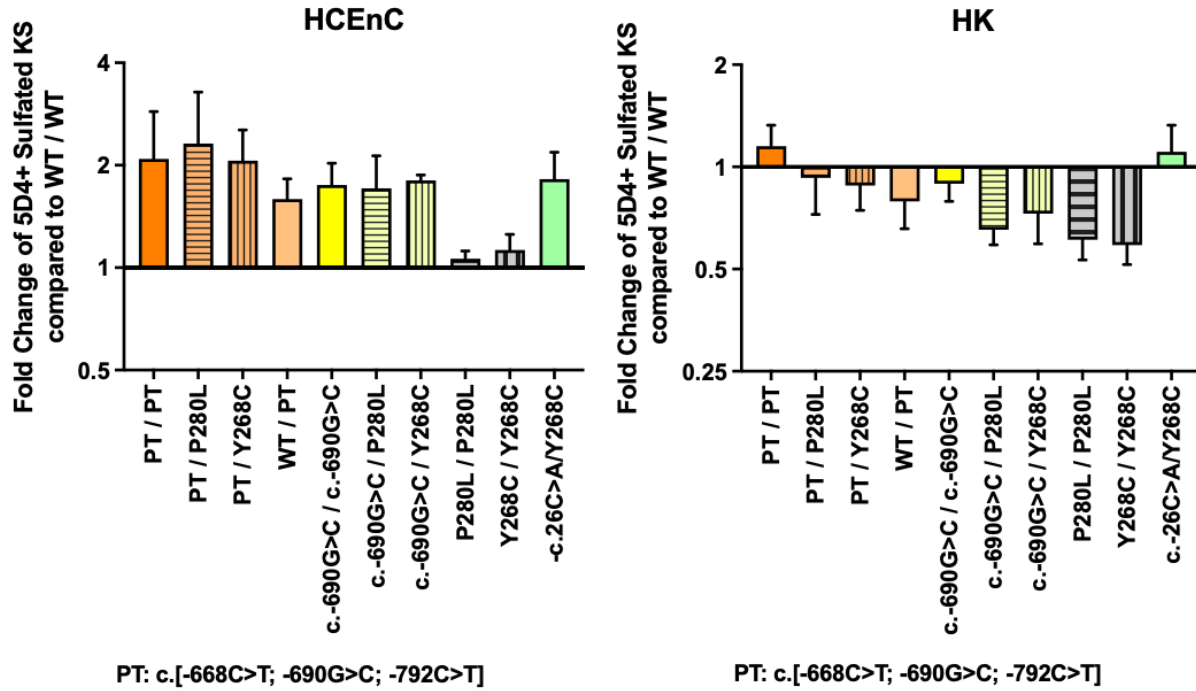
47 20 µg/mL ascorbic acid (Sigma-Aldrich), 10 ng/mL recombinant human fibroblast growth
48 factor (basic), 100 µg/mL penicillin (Thermo Fisher Scientific), and 100 µg/mL
49 streptomycin (Thermo Fisher Scientific). The HCEnC line was maintained in a humidified
50 incubator containing 5% CO₂ at 37°C.

51 *Human corneal keratocyte cell culture*

52 A telomerase immortalized human corneal keratocyte cell line (HK) was cultured in
53 DMEM supplemented with 10% fetal bovine serum (Corning), 100 µg/mL penicillin
54 (Thermo Fisher Scientific), and 100 µg/mL streptomycin (Thermo Fisher Scientific). The
55 HK line was maintained in a humidified incubator containing 5% CO₂ at 37°C.



Supplemental Figure 1. Anterior segment ocular coherence tomography (AS-OCT) images of individuals with Peripheral macular endothelial dystrophy (PMED). (A)
Posterior corneal stromal opacities are observed in the right and left eyes of the proband in Family A. (B) Diffuse stromal edema is present in the right and left eyes of the proband in Family E. (C) Epithelial bullae, subepithelial fibrosis and diffuse stromal edema are present in the right and left eyes of the affected younger sister of the proband in Family E.



Supplemental Figure 2. Functional assay of *CHST6* mutants including previously reported case. Bar graph summary of 5D4+ KS relative fold change in human corneal endothelial cells (HCEnC) or human keratocytes (HK) transfected with mutant CGn6STwPro expression vectors compared to wild-type *CHST6* expression construct (WT/WT). Previously reported compound heterozygous *CHST6* mutations c.-26C>A / c.803A>G, p.(Tyr268Cys) shown as c.- 26C>A/Y268C.²²

Supplemental Table 1. CHST6 screening primer sequences and annealing temperature (T_a)

Gene Region	Forward Primer (5' to 3' Sequences)	Forward Primer (5' to 3' Sequences)	Amplicon Size (bp)	T_a (°C)
Promoter_1	GGTGAGGTGTCTAATGCC	CCCAGGCACCTGAAAAGGAT	861	60
Promoter_2	ATCCTTTCAAGGTGCC	GCACCTGGATGACACATGGA	846	60
Promoter_3	TCCATGTGTCATCCAGGTGC	CTCCCTGGACTCAGCAAAGG	828	65
Exon 1	ACCTTAAGGAGCAAGTCAGCC	CCGCCAAGCTACCGTCTCTC	505	60
Exon 2	CCTGCTTACCAAGGTGCTGA	GAGACTCTGACTCAAAACATACAGT	641	60
Exon 3 – 5CR	GCCCCTAACCGCTGCGCTCTC	GGCTTGCACACGGCCTCGCT	498	68
Exon 3 – MCR	GACGTGTTGATGCCTATCTGCCTTG	TCCGTGGGTGATGTTATGGAT	615	60
Exon 3 – 3CR	CTCCCGGGAGCAGACAGCCA	CTCCCGGGCCTAGCGCCT	599	65
F1 – R1	CCACAGAAGGAAGGACAGAGTAAATGAA	TTCCCTTACTATTATAAAATGCTGCTAATG	N/A	65
F1 – R1M	same as above	TGCTGAATGGCTAACTGAAGGAATACTATAC	N/A	65
F2 – R2	CATATCCTGCTGGCCTAACCTAGTTAC	CATTAGACACCTCACCTGCTTGCG	N/A	65
F2M – R2	CCACAGCCAATTCCATCTGGATTTCTC	same as above	N/A	60

Supplemental Table 2. Candidate variants identified assuming autosomal recessive inheritance

Candidate		dbSNP ID	Family C										Family A				Family B					
Gene	Variant		II-5	III-4	II-7	III-1	II-6	III-2	II-2	II-1	III-5	III-3	II-2	II-1	I-2	I-1	III-1	II-2	II-1	III-1		
<i>SND1</i>	c.1344-7G>A	rs200000137	+/-	+/-	-/-	+/-	-/-	+/-	+/-	+/-	+/-	-/-	No variant in <i>SND1</i> gene									
<i>ANKRD36</i>	c.641_643delTTC	rs367670018	+/-	+/-	-/-	+/-	-/-	-/-	-/-	+/-	-/-	-/-	-/-	-/-	-/-	-/-	-/-	No variants	No variants	No variants		
	c.2307C>G	rs187556886	-/+	-/-	-/-	-/-	-/-	-/+	-/+	-/+	-/+	-/-	-/-	-/-	-/-	-/-	-/-					
	c.1023_1024insGC	rs776547158	-/-	-/-	-/-	-/-	-/-	-/-	-/-	-/-	-/-	-/-	-/-	-/-	-/-	+/-	+/-					
	c.1028_1029del	rs759246247	-/-	-/-	-/-	-/-	-/-	-/-	-/-	-/-	-/-	-/-	-/-	-/-	+/-	+/-	-/-					
	c.1171C>G	rs534738999	-/-	-/-	-/-	-/-	-/-	-/-	-/-	-/-	-/-	-/-	-/-	-/-	+/-	+/-	-/-					
	c.2653+7C>A	rs557559167	-/-	-/-	-/-	-/-	-/-	-/-	-/-	-/-	-/-	-/-	-/-	-/-	+/-	+/-	-/-					
	c.5175dupA	rs132451301	-/-	-/-	-/-	-/-	-/-	-/-	-/-	-/-	-/-	-/-	-/-	-/+	-/-	-/-	-/+					
	c.473T>A	rs200257456	+/-	-/-	-/-	-/-	-/-	-/-	-/-	+/-	-/-	-/-	-/-	-/-	+/-	-/-	-/-	+/-	+/-	-/-		
<i>TAS2R43</i>	c.227A>G	rs11535673	-/+	-/-	-/+	-/+	-/-	-/+	-/-	-/+	-/+	-/-	-/+	-/+	-/+	-/+	-/+	-/+	-/+	-/-		
	c.738G>A	rs199768488	-/-	-/-	-/-	+/-	-/-	-/-	-/-	-/-	-/-	-/-	-/-	+/-	+/-	+/-	+/-	+/-	+/-	-/-		

Supplemental Table 3. Candidate variants identified assuming autosomal dominant inheritance



ICMJE FORM

Date:	8/19/2024
Your Name:	Anthony J Aldave, MD
Manuscript Title:	Peripheral Macular Endothelial Dystrophy: Clinical, Histopathologic, Genetic and Functional Characterization
US-based Author (if yes, you must fill out Open Payment section below):	YES
Manuscript Number (if known):	23-02116

Ophthalmology complies with the position of the International Committee of Medical Journal Editors (ICMJE) on "Conflict of Interest." Conflict of interest for authors is defined as "financial and other conflicts of interest that might bias their work."

In the interest of transparency, we ask you to disclose all relationships/activities/interests listed below that are related to the content of your manuscript. "Related" means any relation with for-profit or not-for-profit third parties whose interests may be affected by the content of the manuscript. Disclosure represents a commitment to transparency and does not necessarily indicate a bias. If you are in doubt about whether to list a relationship/activity/interest, it is preferable that you do so.

The author's relationships/activities/interests should be defined broadly. For example, if your manuscript pertains to the epidemiology of hypertension, you should declare all relationships with manufacturers of antihypertensive medication, even if that medication is not mentioned in the manuscript.

In item #1 below, report all support for the work reported in this manuscript without time limit. For all other items, the time frame for disclosure is the past 36 months.

		Name all entities with whom you have this relationship or indicate none (add rows as needed)	Specifications/Comments (e.g., if payments were made to you or to your institution)
Time frame: Since the initial planning of the work			
1	All support for the present manuscript (e.g., funding, provision of study materials, medical writing, article processing charges, etc.) No time limit for this item.	<input checked="" type="checkbox"/> None <div style="border: 1px solid black; height: 40px; margin-top: 5px;"></div> <div style="border: 1px solid black; height: 40px; margin-top: 5px;"></div> <div style="border: 1px solid black; height: 40px; margin-top: 5px;"></div> <div style="text-align: right; font-size: small;">Click the tab key to add additional rows.</div>	
Time frame: past 36 months			
2	Grants or contracts from any entity (if not indicated in item #1 above).	<input checked="" type="checkbox"/> None <div style="border: 1px solid black; height: 40px; margin-top: 5px;"></div> <div style="border: 1px solid black; height: 40px; margin-top: 5px;"></div> <div style="border: 1px solid black; height: 40px; margin-top: 5px;"></div>	

		Name all entities with whom you have this relationship or indicate none (add rows as needed)	Specifications/Comments (e.g., if payments were made to you or to your institution)								
3	Royalties or licenses	<input checked="" type="checkbox"/> None	<table border="1"> <tr><td></td><td></td></tr> <tr><td></td><td></td></tr> <tr><td></td><td></td></tr> </table>								
4	Consulting fees	<input checked="" type="checkbox"/> None	<table border="1"> <tr><td></td><td></td></tr> <tr><td></td><td></td></tr> <tr><td></td><td></td></tr> <tr><td></td><td></td></tr> </table>								
5	Payment or honoraria for lectures, presentations, speakers bureaus, manuscript writing or educational events	<input checked="" type="checkbox"/> None	<table border="1"> <tr><td></td><td></td></tr> <tr><td></td><td></td></tr> <tr><td></td><td></td></tr> </table>								
6	Payment for expert testimony	<input checked="" type="checkbox"/> None	<table border="1"> <tr><td></td><td></td></tr> <tr><td></td><td></td></tr> <tr><td></td><td></td></tr> </table>								
7	Support for attending meetings and/or travel	<input checked="" type="checkbox"/> None	<table border="1"> <tr><td></td><td></td></tr> <tr><td></td><td></td></tr> <tr><td></td><td></td></tr> </table>								
8	Patents planned, issued or pending	<input checked="" type="checkbox"/> None	<table border="1"> <tr><td></td><td></td></tr> <tr><td></td><td></td></tr> <tr><td></td><td></td></tr> </table>								
9	Participation on a Data Safety Monitoring Board or Advisory Board	<input checked="" type="checkbox"/> None	<table border="1"> <tr><td></td><td></td></tr> <tr><td></td><td></td></tr> <tr><td></td><td></td></tr> </table>								
10	Leadership or fiduciary role in other board,	<input checked="" type="checkbox"/> None	<table border="1"> <tr><td></td><td></td></tr> <tr><td></td><td></td></tr> </table>								

		Name all entities with whom you have this relationship or indicate none (add rows as needed)	Specifications/Comments (e.g., if payments were made to you or to your institution)						
	society, committee or advocacy group, paid or unpaid	<table border="1" style="width: 100%; border-collapse: collapse;"> <tr><td style="height: 40px;"></td><td></td></tr> <tr><td style="height: 40px;"></td><td></td></tr> </table>							
11	Stock or stock options	<input checked="" type="checkbox"/> None <table border="1" style="width: 100%; border-collapse: collapse;"> <tr><td style="height: 40px;"></td><td></td></tr> <tr><td style="height: 40px;"></td><td></td></tr> <tr><td style="height: 40px;"></td><td></td></tr> </table>							
12	Receipt of equipment, materials, drugs, medical writing, gifts or other services	<input checked="" type="checkbox"/> None <table border="1" style="width: 100%; border-collapse: collapse;"> <tr><td style="height: 40px;"></td><td></td></tr> <tr><td style="height: 40px;"></td><td></td></tr> <tr><td style="height: 40px;"></td><td></td></tr> </table>							
13	Other financial or non-financial interests	<input checked="" type="checkbox"/> None <table border="1" style="width: 100%; border-collapse: collapse;"> <tr><td style="height: 40px;"></td><td></td></tr> <tr><td style="height: 40px;"></td><td></td></tr> <tr><td style="height: 40px;"></td><td></td></tr> </table>							

Please place an "X" next to the following statement to indicate your agreement:

I certify that I have answered every question and have not altered the wording of any of the questions on this form.

FOR US-BASED AUTHORS ONLY>>> [OPEN PAYMENTS](#)

For US-based authors (i.e., those with a US National Provider Identifier [NPI]), it is now required they look up their [Open Payments](#) record (past 2 years only) to confirm that it matches what is reported on the ICMJE Form. If there are discrepancies, the co-author must provide a brief explanation on the ICMJE Form along with the Open Payment URL person record (e.g., <https://openpaymentsdata.cms.gov/physician/1316209>). To learn more about this new requirement, please refer to [Van Gelder RN and Siegfried CJ. ROI, COI, and the Ethical Obligations of Journals. Ophthalmology. 2022; 129: 602-604.](#)

Open Payments URL:	https://openpaymentsdata.cms.gov/physician/332105
<hr/>	
Match Disclosure Form?	YES
<hr/>	
If no, please briefly explain discrepancy:	Click or tap here to enter text.
<hr/>	

Wenlin Zhang, M.D., Ph.D., is currently a resident physician in Medical Genetics at UCLA Medical Center and an aspiring physician-scientist. She earned a Ph.D. in Vision Science and completed postdoctoral training in ophthalmic genetics at the Stein Eye Institute. Dr. Zhang is a prolific author, a recipient of multiple competitive research grants, and a co-inventor on several patents. She is dedicated to advancing precision medicine through translational research.

